Taxonomia integrativa das espécies de *Myloplus* (Characiformes: Serrasalmidae) da bacia do Prata

Victória Dandara Pereira e Silva

Botucatu, SP

2024

Universidade Estadual Paulista "Júlio de Mesquita Filho"Instituto de Biociências de Botucatu

Taxonomia integrativa das espécies de *Myloplus* (Characiformes: Serrasalmidae) da bacia do Prata

Aluna: Victória Dandara Pereira e Silva

Orientador: Prof. Dr. Claudio Oliveira

Coorientador: Profª. Draª. Rafaela Priscila Ota

Dissertação apresentada ao Instituto de Biociências, Campus de Botucatu, UNESP, para defesa de Mestrado no Programa de Pós-Graduação em Ciências Biológicas (Zoologia).

Botucatu, SP

2024

FICHA CATALOGRÁFICA ELABORADA PELA SEÇÃO TÉC. AQUIS. TRATAMENTO DA INFORM.
DIVISÃO TÉCNICA DE BIBLIOTECA E DOCUMENTAÇÃO - CÂMPUS DE BOTUCATU - UNESP
BIBLIOTECÁRIA RESPONSÁVEL: ROSANGELA APARECIDA LOBO-CRB 8/7500

Silva, Victória Dandara Pereira e.
Taxonomia integrativa das espécies de *Myloplus* (Characiformes: Serrasalmidae) da bacia do Prata / Victória Dandara Pereira e Silva. - Botucatu, 2024

Dissertação (mestrado) - Universidade Estadual Paulista (UNESP), Instituto de Biociências, Botucatu
Orientador: Claudio de Oliveira
Coorientador: Rafaela Priscila Ota
Capes: 20405006

1. Pacu (Peixe). 2. Characídeos. 3. Taxonomia (Zoologia). 4. Genes mitocondriais. 5. Marcadores genéticos.

Palavras-chave: COI; Myleinae; Neotropical; Pacu; Serrasalmidae.

Taxonomia integrativa das espécies de *Myloplus* (Characiformes: Serrasalmidae) da bacia do Prata

Aluna: Victória Dandara Pereira e Silva

Orientador: Prof. Dr. Claudio Oliveira

Coorientador: Profª. Draª. Rafaela Priscila Ota

Dissertação apresentada ao Instituto de Biociências, Campus de Botucatu, UNESP, para defesa de Mestrado no Programa de Pós-Graduação em Ciências Biológicas (Zoologia).

Data de aprovação: 29/05/2024

BANCA EXAMINADORA

Prof. Dr. CLAUDIO DE OLIVEIRA (Participaçao Presencial)
Departamento de Zoologia / Universidade Paulista "Júlio de Mesquita Filho", Instituto de Biociências da Unesp de Botucatu

Profa. Dra. NADAYCA THAYANE BONANI MATEUSSI (Participaçao Virtual)
-
Prof. Dr. RICARDO CARDOSO BENINE (Participaçao Presencial)
Departamento de Zoologia / Universidade Paulista "Júlio de Mesquita Filho", Instituto de Biociências da Unesp de Botucatu

Botucatu, SP

2024

Esta pesquisa foi financiada com recursos da Coordenação de Aperfeiçoamento de Pessoal de Nível Superior (CAPES)

Agora e sempre, às grandes mulheres da minha vida:

Geni, Ester, Jacy, Andrea, Sueli e Vanessa.

Agradecimentos

Agradeço ao meu orientador, Prof. Claudio Oliveira, por aceitar me orientar, por sua constante presença e dedicação, e por sua humanidade e respeito, que me inspiram tanto como pesquisadora quanto como ser humano.

Agradeço também à minha coorientadora, Profª. Rafaela Ota, que me acompanha desde minha primeira iniciação científica, que como diz o poeta: "Que já viajou tantas canções comigo e ainda há tantas por viajar". Que me inspira como cientista e mulher independente, inteligente e forte.

Agradeço especialmente aos amigos de laboratório: Mariana Kuranaka, Giovanna Ribeiro, Aisni Mayumi, Thiago Farias e Jefferson Crispim, que me auxiliaram e ensinaram diversas técnicas, desde as de bancada até análises filogenéticas e muito mais, contribuindo diretamente para o desenvolvimento desse trabalho.

Agradeço a todos, sem exceção, do Laboratório de Biologia e Genética de Peixes, que também contribuíram significativamente com aprendizados acadêmicos e de vida durante esses anos de mestrado.

Agradeço aos meus amigos de Manaus do INPA e da Ufam, pelos quais tenho grande carinho, especialmente Lúcia, Marcelo, Renildo, Alany, Valéria, Isaac, Gabriel, Isabel e Douglas.

Agradeço às minhas amigas-irmãs, Vanessa, Kate e Gab.

Agradeço aos meus familiares, em especial à minha tia Andrea, meus avós, Sueli e Waldemar, e meu pai, Adriano, por todo o suporte e cuidado ao longo da vida. Agradeço com carinho ao meu parceiro, Gabriel, por todos os momentos e ensinamentos partilhados.

Agradeço ao Instituto de Biociências de Botucatu, ao programa de Pós-graduação em Zoologia e aos funcionários do Departamento de Biologia Estrutural e Funcional e da seção técnica de Pós-graduação, cujo trabalho permitiu a realização deste estudo.

"Tenho em mim um sentimento de aldeia e dos primórdios.

Eu não caminho para o fim, eu caminho para as origens."

Manoel de Barros

Resumo

Myloplus possui, atualmente, 15 espécies válidas, das quais, apenas *M. tiete* e *M. levis* ocorrem no sistema Paraná-Paraguai. Ambas são descritas com base em apenas um espécime e possuem descrições originais breves, tendo *M. levis* já sido considerada um sinônimo júnior de *M. tiete.* Filogenias moleculares recentes sugerem que as duas espécies são proximamente relacionadas. Para verificar se essas duas espécies realmente correspondem a táxons distintos, conduzimos uma abordagem integrativa, usando análises morfológicas e moleculares (COI). Nossos resultados demonstraram que *M. tiete* e *M. levis* são espécies distintas. *Myloplus tiete* pode ser diagnosticado de *M. levis* por: maior distância entre o término da nadadeira dorsal até o término da nadadeira anal (21,8–25,3% SL *vs*. 17,0–20,0), base da nadadeira adiposa mais longa (4,1–5,8% SL *vs*. 2,6–3,8), último raio da nadadeira anal curto e estreito (*vs*. longo e largo) e espinhos da quilha ventral curtos (*vs*. longos). Resultados moleculares recuperaram as espécies como táxons distintos, com distância interespecífica de 8,5%. Por hora, a atual classificação de *M. tiete* como uma espécie ameaçada (EN) de acordo com os critérios da IUCN pode ser devido à falta de uma definição apropriada da espécie. Esse estudo demonstra como a aplicação de abordagens integrativas podem ser úteis para melhorar a compreensão de táxons com históricos taxonômicos complexos, com descrições originais insuficientes e com grande similaridade morfológica.

Palavras-chave. COI, Myelinae, Neotropical, Pacu, Serrasalmidae.

Abstract

Of the 15 species of *Myloplus,* only *M. tiete* and *M. levis* occur in Paraná-Paraguay River Basin. Each of the two species was briefly described based on a single specimen, and thus the diagnostic characters of *M. tiete* and *M. levis* are not clearly stated in the literature, which led to *M. levis* being sometimes considered a junior synonym of *M. tiete*. Recent molecular phylogenies suggested that the two species are very closely related. To verify if these two species correspond to distinct taxa, we carried out an integrative analysis using morphological and molecular (COI) data. Our results demonstrate that *M. tiete* and *M. levis* are two different species. *Myloplus tiete* can be diagnosed from *M. levis* by: longer dorsal-fin terminus to anal-fin terminus distance (21.8–25.3% SL *vs*. 17.0–20.0), longer adipose-fin base (4.1–5.8% SL *vs*. 2.6–3.8), the last anal-fin unbranched ray short and narrow (*vs*. long and wide), and short ventral-keel spines (*vs*. long). Molecular results also identified the species as distinct taxa, with an interspecific distance of 8.5%. Currently, *M. tiete* is categorized as Endangered (EN) according to IUCN criteria. This study demonstrates how the application of integrative approaches can be useful for a better understanding of taxa with complex taxonomic history, uninformative original descriptions, and significant morphological similarity.

Key words. COI, Myelinae, Neotropical, Pacu, Serrasalmidae.

Sumário

Introdução

A ordem Characiformes, compreendendo 289 gêneros distribuídos em 24 famílias (Fricke, Eschmeyer, Fong, 2024), constitui um dos grupos morfologicamente mais variados entre os peixes de água doce, o que permitiu sua adaptação a diferentes nichos tróficos e ambientais na região Neotropical e na África (Betancur *et al*., 2019; Burns, Sidlauskas, 2019; Ohara *et al*., 2017). Dentre as famílias neotropicais, encontra-se Serrasalmidae, que abriga peixes de grande importância comercial, popularmente conhecidos como pacus, piranhas, o tambaqui e a pirapitinga (Ota *et al*., 2013). A família apresenta grande diversidade morfológica e atualmente é composta por 18 gêneros (Fricke, Eschmeyer, Fong, 2024), sendo um deles o gênero fóssil *Megapiranha* Cione *et al.*, 2009.

Quanto às relações filogenéticas dentro de Serrasalmidae, as mais recentes filogenias publicadas sugerem a divisão da família em dois ou três grandes grupos. A hipótese filogenética proposta por Mateussi *et al*. (2020), utilizando elementos ultraconservados, recupera duas subfamílias: Colossomatinae e Serrasalminae, sendo a última subdivida em duas tribos de acordo com o tipo de espinho pré-dorsal, Myleini, composta pelos pacus com espinho contínuo ao primeiro pterigióforo, e Serrasalmini, composta por *Metynnis* Cope, 1878 e as piranhas com espinho descontínuo. Já a hipótese proposta por Kolmann *et al*. (2020), utilizando éxons, recupera três subfamílias: Colossomatinae, Myleinae e Serrasalminae. A única diferença entre as propostas é o método de classificação utilizado, subordinação na primeira e sequenciamento na segunda.

Dentro de Myleinae (*sensu* Kolmann *et al*., 2020) ou Myleini (*sensu* Mateussi *et al*., 2020), *Myloplus* Gill, 1896 é o gênero com o maior número de espécies, atualmente composto por 15 espécies válidas. Os representantes do gênero são pacus de médio a grande porte que habitam diversos tipos de ambientes, desde lagos com águas lentas até corredeiras e pequenas quedas d'água (Jégu, 2003; Andrade *et al*., 2016).

Embora atualmente muitas espécies sejam atribuídas a *Myloplus*, seu histórico taxonômico é bastante complexo. *Myloplus* foi originalmente proposto por Gill (1896) como subgênero de *Myleus* (*sensu* Müller, Troschel, 1844), que então era composto por dois subgêneros, *Myleus* e *Myletes*. Gill (1896), através de uma breve menção em único parágrafo, sem fornecer descrição complementar ou indicar espécie tipo, propôs *Myloplus*

como substituto de *Myletes sensu* Müller, Troschel (1844), pois *Myletes sensu* Cuvier (1816) já estava em uso para outra espécie não relacionada. Dessa forma *Myletes* foi substituído (e posteriormente suprimido) por *Myloplus*, que por sua vez foi considerado subgênero ou sinônimo júnior de *Myleus* por mais de um século (Eigenmann, 1910, 1912; Géry, 1972).

Eigenmann (1912), ao analisar peixes da Guiana Inglesa, indica *Myletes asterias* Müller, Troschel, 1844 como espécie tipo do subgênero *Myloplus*. No entanto, por muitos anos as características indicadas para esta espécie foram consideras insuficientes para sua diagnose, tendo sido considerada um sinônimo júnior de *Myletes rubripinnis* Müller, Troschel, 1844. Jégu *et al.* (2004) ao analisarem material tipo das espécies realocadas, *Myleus asterias* e *Myleus rubripinnis*, além de material complementar oriundo das Guianas e do rio Amazonas, foram capazes de separar adequadamente as duas espécies e assim revalidar a espécie tipo de *Myloplus*. Além disso, os autores também identificaram características que diagnosticavam *Myloplus*, elevando-o à categoria de gênero.

Sobre o relacionamento das espécies, a filogenia proposta por Kolmann *et al*. (2020), recuperou *Myloplus* como parafilético e propôs novos arranjos taxonômicos. Dois subgêneros de *Myleus* foram revalidados para alocar três espécies anteriormente posicionadas em *Myloplus* [*i.e*. *Prosomyleus* Géry, 1972, para alocar *P. rhomboidalis* (Cuvier, 1818), e *Paramyloplus* Norman, 1929, para alocar *P. ternetzi* Norman, 1929 e *P. taphorni* (Andrade *et al*., 2019)]. No entanto, nenhuma diagnose morfológica foi fornecida para nenhum dos gêneros. Ainda no mesmo trabalho, *Myloplus planquettei* Jégu, Keith, Le Bail 2003 foi transferida para *Myleus planquettei*. Mesmo considerando esses rearranjos *Myloplus* permaneceu parafilético.

Mateussi *et al*. (2020) utilizaram um número maior de espécies de Serrasalmidae em sua análise filogenética, mas também não recuperaram a monofilia de *Myloplus*, com espécies proximamente relacionadas a outros gêneros (*e.g. Myleus*, *Mylesinus* Valenciennes, 1850, *Tometes* Valenciennes, 1850 e *Utiaritichthys* Miranda Ribeiro, 1937). O problema central consiste na diagnose desses gêneros, baseada na forma e distribuição dos dentes do pré-maxilar (Géry, 1972; Jégu *et al*., 2003, 2004), caráter que vem se demonstrando homoplástico nas últimas análises filogenéticas da família (Orti *et al*., 2008; Thompson *et al*., 2014; Kolmann *et al*., 2020; Mateussi *et al*., 2020). Além disso, as espécies exibem grande variação morfológica associada à ontogenia e dimorfismo sexual, o que dificulta o reconhecimento dos limites intra- e interespecíficos (Machado *et al*., 2018; Ota *et al*., 2020).

Taxonomia Integrativa e DNA barcoding

A taxonomia clássica baseada em caracteres estritamente morfológicos possui limitações atualmente muito discutidas, entre elas: necessidade de especialistas para correta identificação de táxons; existências de espécies crípticas (que não são distintas morfologicamente); descrições originais insuficientes e séries tipo perdidas; grande plasticidade fenotípica intraespecífica; dificuldade de identificação morfológica correta ao longo de toda ontogenia dos táxons (Pires, Marinoni, 2010). Assim, a junção de mais de uma, ou até a aplicação de várias técnicas de análises diferentes, tem sido muito utilizada para alcançar um melhor entendimento sobre a biodiversidade. A utilização dessa abordagem é conhecida como taxonomia integrativa (Dayrat, 2005).

Embora muitas outras metodologias possam ser utilizadas, as análises moleculares têm sido uma ferramenta muito importante para a delimitação de táxons e para o avanço do entendimento sobre as relações filogenéticas das espécies. Com a criação da técnica de PCR (Polymerase Chain Reaction) para amplificação do DNA, tornou-se possível a delimitação de espécies com base apenas no sequenciamento de um determinado trecho de DNA amplificado. A técnica recebe o nome de DNA barcoding em referência direta ao código de barras, uma vez que cada ser vivo apresenta uma sequência de DNA diferente, podendo assim ser identificado apenas com base na leitura desse código (Hebert *et al*., 2003).

O DNA barcoding é realizado em um trecho específico no DNA mitocondrial, uma pequena região no gene citocromo c oxidase subunidade I (COI) de cerca de 650 pares de bases. A escolha do gene está principalmente relacionada à possibilidade de reconhecimento de espécies crípticas e estruturação filogeográfica das espécies, uma vez que possui uma grande amplitude de sinal filogenético, apresentando substituições nucleotídicas mais rápidas, além disso, o gene possui primers universais que permitem o sequenciamento de quase todos os filos e *indels* (inserções/deleções) raros (Hebert *et al*., 2003).

Assim, a identificação de espécies através de análises de DNA, como a técnica de DNA barcoding, contorna alguns problemas centrais da taxonomia clássica como: facilitar a identificação de qualquer táxon em qualquer estágio de vida, mesmo larvas e

juvenis, e tornar possível a delimitação de espécie morfologicamente crípticas. No entanto, ressalta-se que o DNA barcoding identifica espécies através da comparação de sequências previamente analisadas e depositadas em um banco de dados, como o GenBank e o BOLD. Neste caso, mesmo que seja possível a identificação de espécies no banco através apenas de amostras de tecido, também há a necessidade de manter os exemplares testemunhos para realização de análises morfológicas e estudos taxonômicos detalhados (Pires, Marinoni, 2010).

No trabalho de DNA barcoding mais abrangente utilizando representantes de Serrasalmidae, Machado *et al*. (2018) focaram na grande diversidade amazônica e demonstraram que a riqueza de espécies dentro da família ainda é muito subestimada. Nesse trabalho, 13 espécies até então consideras pertencentes a *Myloplus* foram incluídas e o gênero foi recuperado parafilético.

Bacia do Prata

A bacia do Prata é composta por três principais sub-bacias, Paraguai, Paraná e Uruguai e possui cerca de 3,1 milhões de km² de extensão, consistindo na segunda maior bacia da América do Sul. A bacia do Prata banha cinco países, Brasil, Paraguai, Uruguai, Bolívia e Argentina, abrigando uma importante e extensa área alagada no Brasil, o Pantanal (Villar *et al*., 2018; Reis *et al*., 2016). Por ocupar uma região que envolve cinco países, conflitos quanto a gestão e conservação dos recursos hídricos e da biodiversidade são constantes. A área é densamente povoada e possui grande importância econômica principalmente relacionada à geração de energia hidroelétrica (Villar *et al*., 2018).

A presença destas hidrelétricas acarreta uma série de impactos ambientais nesta bacia e afeta diretamente sua ictiofauna (Fráguas, Pompeu, 2021). Um grande exemplo é a usina hidrelétrica de Itaipu, cuja construção inundou uma ampla área no alto rio Paraná, região do Salto das Sete Quedas, que atuava como uma barreira natural para espécies de peixes deste rio. Sua inundação ocasionou a remoção dessa barreira e, dessa forma, algumas espécies que antes eram endêmicas do baixo rio Paraná puderam colonizar o alto Paraná (Reis *et al*., 2020). Outro exemplo, é a UHE de Yacyretá, que está localizada próxima à divisa entre Paraguai e Argentina, cuja implantação causou grande impacto na ictiofauna local levando à diminuição do estoque pesqueiro e ao desaparecimento de algumas espécies na região (Ulloa, Bellini, 2009).

A bacia do Prata consiste na terceira bacia mais diversa em peixes de água doce

da América do Sul. Possuindo representantes de 44 famílias, 242 gêneros e cerca de 924 espécies, das quais 444 são consideradas endêmicas (Reis et al, 2016). Entre os representantes da bacia, destacam-se o *Salminus brasiliensis* (Cuvier, 1816), popularmente conhecido como dourado e a importante espécie comercial *Prochilodus lineatus* (Valenciennes, 1837), popularmente conhecida como curimba.

Sobre as espécies de *Myloplus* presentes na bacia do Prata, *M. tiete* (Eigenmann, Norris 1900) e *M. levis* (Eigenmann, McAtee 1907) possuem ocorrência conhecida para as sub-bacias Paraná-Paraguai, não havendo registros para sub-bacia do rio Uruguai. Sabe-se que a presença dos diversos barramentos na bacia do Prata consiste em uma ameaça para as espécies que habitam ambientes lóticos, entre elas *Myloplus tiete*, que possui distribuição indicada para bacia dos rios Paraná, mas que atualmente é considerada rara no alto rio Paraná, sendo encontrada mais frequentemente em determinados locais, como Ivinhema, Piquiri e Iguatemi (Akama *et al*., 2018).

Objetivos

Geral

- Testar a hipótese da existência de uma única espécie de *Myloplus* para a bacia do Prata através de uma revisão taxonômica integrativa.

Específicos

- Obter dados moleculares de amostras de especimes de *Myloplus* da bacia do Prata.
- Obter dados morfológicos e merísticos de amostras de *Myloplus* de toda a bacia do Prata.
- Integrar os dados obtidos descrevendo formalmente os táxons identificados para a bacia do Prata.

Os materiais e métodos utilizados, bem como os resultados obtidos e sua discussão, serão apresentados a seguir em um capítulo estruturado na forma de um artigo científico

Referências

Fricke R, Eschmeyer WN, Fong JD. Eschmeyer's catalog of fishes: genera, specie by family/subfamily [Internet]. San Francisco: California Academy of Science; 2024.

Fricke R, Eschmeyer WN, Van der Laan R. Eschmeyer's catalog of fishes: genera, species, references [Internet]. San Francisco: California Academy of Science; 2024.

Géry J. Poissons Characoïdes des Guyanes. I. Généralités. II. Famille des Serrasalmidae. Zool Verh. 1972. 122(1): 1–250. http://www.repository.naturalis.nl/record/317730%5Cnhttp://www.repository.naturalis.nl/document/149016

Gill NT. Note on the fshes of the genus Characinus. Proc U S Natl Mus. 1896; 18(1058):213–215. https://doi.org/10.5479/si.00963801.18-1058.213

Hebert PDN, Cywinska A, Ball SL, Ward JR. Biological identifications through DNA barcodes. P Roy Soc Lond B. 2003; 270:313–321.

Jégu M. Subfamily Serrasalminae (Pacus and Piranhas). In: Reis RE, Kullander SO, Ferraris CJ, Jr., editors. Check list of the freshwater fishes of South and Central America. Porto Alegre: Edipucrs; 2003. p.182–96.

Jégu M, Hubert N, Belmont-Jegu E. Réhabilitation de *Myloplus asterias* (Müller & Troschel, 1844), espèce-type de *Myloplus* Gill, 1896 et validation du genre *Myloplus* Gill (Characidae: Serrasalminae). Cybium. 2004; 28(2):119–57. https://doi.org/10.26028/cybium/2004-282-005

Kolmann MA, Hughes LC, Hernandez LP, Arcila D, Betancur-R R, Sabaj MH *et al*. Phylogenomics of piranhas and pacus (Serrasalmidae) uncovers how dietary convergence and parallelism obfuscate traditional morphological taxonomy. Syst Biol. 2020; 70(3):576–92. https://doi.org/10.1093/sysbio/syaa065

Machado VN, Collins RA, Ota RP, Andrade MC, Farias IP, Hrbek T. One thousand DNA barcodes of piranhas and pacus reveal geographic structure and unrecognized diversity in the Amazon. Sci Rep. 2018; 8:8387. https://doi.org/10.1038/ s41598-018-26550-x

Mateussi NTB, Melo BF, Ota RP, Roxo FF, Ochoa LE, Foresti F *et al*. Phylogenomics of the Neotropical fish family Serrasalmidae with a novel intrafamilial classification (Teleostei: Characiformes). Mol Phylogenet Evol. 2020; 153:106945. https://doi.org/10.1016/j.ympev.2020.106945

Ohara WM, Lima FCT, Salvador GN, Andrade MC. Peixes do rio Teles Pires: Diversidade e guia de identificação. Aparecida de Goiânia: Gráfica Amazonas e Editora Ltda; 2017.

Ortí G, Sivasundar A, Dietz K, Jégu M. Phylogeny of the Serrasalmidae (Characiformes) based on mitochondrial DNA sequences. Genet Mol Biol. 2008; 31(1):343–51. https://www.scielo.br/j/gmb/a/WQBqC6FyNFCmFPqwN8jmXXh/?format=pdf&lang=en

Ota RP, Röpke CP, Zuanon JAS, Jégu M. Peixes do rio Madeira, volume II, a ictiofauna do rio Madeira. Itupeva: Dialeto Latin American Documentary; 2013

Ota RP, Machado VN, Andrade MC, Collins RA, Farias IP, Hrbek T. Integrative taxonomy reveals a new species of pacu (Characiformes: Serrasalmidae: *Myloplus*) from the Brazilian Amazon. Neotrop Ichthyol. 2020; 18(1):e190112. https://doi.org/10.1590/1982-0224-20190112

Pires AC, Marinoni L. DNA barcoding and traditional taxonomy unified through integrative Taxonomy: A view that challenges the debate questioning both methodologies. Bio Neotrop. 2010; 10(2):339–346. https://doi.org/10.1590/S1676-06032010000200035

Reis RE, Albert JS, Di Dario F, Mincarone MM, Petry P, Rocha LA. Fish biodiversity and conservation in South America. J Fish Biol. 2016; 89(1): 12–47. https://doi.org/10.1111/jfb.13016

Reis BR, Augusto F, Deprá GC, Ota RR, Weferson JG. Freshwater fishes from Paraná State, Brazil: an annotated list, with comments on biogeographic patterns, threats, and future perspectives. 2020; 4868(4): 451–494. https://doi.org/10.11646/zootaxa.4868.4.1

Thompson AW, Betancur-RR, López-Fernández H, Ortí G. A time-calibrated, multi-locus phylogeny of piranhas and pacus (Characiformes: Serrasalmidae) and a comparison of species tree methods. Mol Phylogenet Evol. 2014; 81:242–57. http://dx.doi.org/10.1016/j.ympev.2014.06.018

Ulloa V, Bellini LM. A usina hidrelétrica de Yacyretá: insustentabilidade e exclusão social no rio Paraná (Corrientes, Argentina). Sociedade & Natureza. 2009; 21(3): 373–391. https://doi.org/10.1590/S1982-45132009000300012

Villar PC, Ribeiro WC, Sant'Anna FM. Transboundary governance in the La Plata River basin: status and prospects. Water Int. 2018; 43(7): 978–995. https://doi.org/10.1080/02508060.2018.1490879

Capítulo 1. Redescription of *Myloplus* (Characiformes: Serrasalmidae) from La Plata Basin

Capítulo 1 - Redescription of *Myloplus* (Characiformes: Serrasalmidae) from La Plata Basin

1.1 Introduction

The vernacular name "pacu" commonly refers to freshwater Neotropical fishes of the subfamily Myleinae *sensu* Kolmann *et al*. (2020), which currently comprises nine genera, *viz*. *Myleus* Müller, Troschel, 1844; *Myloplus* Gill, 1896; *Mylesinus* Valenciennes, 1850; *Tometes* Valenciennes, 1850; *Acnodon* Eigenmann, 1903; *Paramyloplus* Norman, 1929; *Utiaritichthys* Miranda Ribeiro, 1937; *Prosomyleus* Géry, 1972; and *Ossubtus* Jégu, 1992. This composition is very similar to Myleini *sensu* (Mateussi *et al*., 2020), with the exception of *Paramyloplus* and *Prosomyleus*, which are considered junior synonyms of *Myleus*. To date, the distinction between these genera is primarily based on morphological characteristics, often associated with the neurocranium and dentition.

Although these morphological characters are still widely used to separate the genera, recent molecular studies (Machado *et al*., 2018; Ota *et al*., 2020; Mateussi *et al*., 2020; Kolmann *et al*., 2020) demonstrated the polyphyletic nature of almost all genera within Myleinae. These studies demonstrate that these morphological characteristics are the result of adaptive convergences (Goulding, 1980; Kolmann *et al*., 2020) and do not serve the purpose of defining monophyletic groups.

Among the genera of Myleinae, *Myloplus* is the most species-rich group, currently composed of 15 species [*i.e*., *M. animacula* Soares *et al*., 2023; *M. arnoldi* Ahl, 1936; *M. asterias* (Müller, Troschel, 1844); *M. levis* (Eigenmann, McAtee, 1907); *M. lobatus* (Valenciennes, 1850); *M. lucienae* Andrade *et al*., 2016; *M. nigrolineatus* Ota *et al*., 2020; *M. rubripinnis* (Müller, Troschel, 1844); *Myloplus aylan* Pereira *et al*., 2024, in press; *Myloplus sauron* Pereira *et al*., 2024; *M. schomburgkii* (Jardine, 1841); *M. tiete* (Eigenmann, Norris, 1900); *M. torquatus* (Kner, 1858); *M. tumukumak* Andrade *et al*., 2018; and *M. zorroi* Andrade, Jégu, Giarrizzo, 2016]. Like other genera in the subfamily, it is diagnosed by morphological characteristics mainly involving dentition, *e.g*., premaxilla with molariform teeth arranged in two rows, spaced by an internal gap between them; lack of contact in the symphysis of premaxillary teeth of contralateral labial rows, and is recovered in molecular phylogenies as polyphyletic.

While molecular analyses have emphasized the limited knowledge about the generic relationships of Myleinae, the application of integrative taxonomy has helped

reveal its cryptic diversity (Andrade *et al*., 2017; Escobar *et al*., 2019; Ota *et al*., 2020). Of the 15 species of *Myloplus*, seven were described in the past decade, all from the Amazon region, where the greatest taxonomic efforts are concentrated (Andrade *et al*., 2016a,b, 2018; Ota *et al*., 2020; Soares *et al*., 2023; Pereira *et al*., 2024, in press). Although the genus reaches its peak diversity in this region, two poorly studied species, *Myloplus tiete* and *M. levis*, are known from the La Plata River basin.

Myloplus tiete the only species of *Myloplus* known in the upper Paraná basin, has "Piracicaba" (Piracicaba municipality, São Paulo state) as its type locality, without precise information. The species was described based only on the holotype, a juvenile specimen, which is currently lost. *Myloplus levis*, on the other hand, was described from "Bahia Negra", in the Paraguay River basin, also based on a single specimen, but preserved at the California Academy of Sciences (CAS, catalog number 62107). Although the two species were described from different portions of the La Plata River basin, the lack of a holotype of *M. tiete* and the poorly detailed description of both species perpetuate taxonomic uncertainties.

In 1951, Gosline considered *M. levis* a junior synonym of *M. tiete*, claiming that there had been no comparison between the two species until then. Only decades later, Jégu (2003) recognized the species as distinct taxa; however, he did so in a species catalog and did not offer new diagnostic characteristics (Reis *et al*., 2003). Recently, with the use of molecular analyses involving the mitochondrial gene cytochrome c oxidase subunit I (COI) and ultraconserved elements of genome (UCEs), specimens identified as *M. tiete* and *M. levis* were recovered as closely related (Machado *et al*., 2018; Mateussi *et al*., 2020), even having the same haplotype in COI sequences (Machado *et al*., 2018).

In the absence of a taxonomic review study, the two species are identified mainly based on geographical distribution, although specimens collected in the lower Paraguay and lower Paraná have been erroneously identified as *M.* cf. *asterias* and *M. tiete* (Campos, 1945). Furthermore, fish collections often contain specimens identified as *M. tiete* from the Paraguay basin and as *M. levis* from the Paraná basin.

Another crucial point is that due to the impacts of many barriers created by hydroelectric power plants on the upper Paraná River basin, as the greatest example of Itaipu hydroelectric power plant, that allowed that species from lower Paraná moves to upper Paraná region, many of the native species the inhabits the upper Paraná basin are currently strongly threatened, as in the case of *Myloplus tiete*, that is considered Endangered (EN) according to the IUCN Red List criteria (Akama *et al*., 2018).

Considering the taxonomic uncertainty involving these species, we used integrative taxonomy to investigate whether *Myloplus levis* and *M. tiete* differ from each other and from their congeners. The main results were: (1) COI results recovered *M. levis* and *M. tiete* as distinct evolutionary lineages, and our morphological analyses corroborate this, revealing numerous diagnostic characteristics between these species. (2) During the review, we identified a different *Myloplus levis* morphotype that could represent a different species. (3) We were able to verify morphologically and generate sequence data for the recently described species, *M. animacula*, demonstrating its close relationship with *M. levis*. (4) We detected a new "*Myloplus*" lineage from the Tocantins River basin, which does not correspond to any sampled lineage.

1.2 Material and Methods

1.2.1 Morphological analysis

Counts and measurements were taken according to Machado *et al*. (2024). Measurements, which are presented as percentages of standard length (SL) and head length (HL), were taken with a digital caliper to the nearest 0.1 mm between landmarks. Counts were taken under a stereomicroscope. The count of ventral keel spines is composed of prepelvic spines (all those preceding the pelvic-fin insertion), postpelvic spines (those between a vertical through the pelvic-fin insertion and the anus), and the paired spines lateral to the anus. Osteological terminology follows Mattox *et al*. (2014). Counts of vertebrae, supraneurals, pterygiophores, and ventral keel spines, as shape and position of these osteological structures were obtained from radiographed specimens and from tomography. Vertebrae counts include those of the Weberian apparatus as four elements, and the fused PU1+U1 as a single centrum. In the descriptions, counts of the numbers in parentheses indicate the frequency of the counts. In the analyzed material lists, the total number of specimens is followed by tissue voucher number in parentheses. Institucional abreviativos are: DZSJRP, Departamento de Zoologia e Botânica, Universidade Estadual Paulista "Júlio de Mesquita Filho", São José do Rio Preto, São Paulo; LBP, Laboratório de Biologia e Genética de Peixes, Instituto de Biociências, Unesp, Botucatu, São Paulo; MNRJ, Museu Nacional, Universidade Federal do Rio de Janeiro, Rio de Janeiro; MZUSP, Museu de Zoologia da Universidade de São Paulo, São Paulo; NUP, Coleção Ictiológica do Núcleo de Pesquisas em Limnologia, Ictiologia e

Aquicultura, Maringá, Paraná; ZUEC, Museu de Zoologia da Universidade Estadual de Campinas "Adão José Cardoso", Campinas, São Paulo.

1.2.2 Molecular analysis

For the molecular analyses we used 55 available COI sequences from the GenBank nucleotide (https://www.ncbi.nlm.nih.gov/nucleotide) database (Tab. S1), that were published in previous studies (Machado *et al*., 2018, 2024 *in press*; Ota *et al*., 2020; Papa *et al*., 2021), including those identified as "*Myloplus tiete*" and "*M. levis"*. We also generated 19 new COI sequences from specimens of *Myleus* from Tocantins-Araguaia, Paraguay, and Paraná basins (Tab. 1). Due to the polyphyletic nature of the genus, beside all the species of *Myloplus* we also included representatives of another Myleinae (*sensu* Kolmann *et al*., 2020) genera (*i.e*. *Acnodon*, as out group; *Myleus*; *Ossubtus*; *Paramyloplus*; *Prosomyleus* and *Tometes*). Twelve of the 15 valid species of *Myloplus* were included, (*i.e. M. arnoldi*, *M. asterias*, *M. aylan*, *M. levis*, *M. lobatus*, *M. lucienae*, *M. nigrolineatus*, *M. rubripinnis*, *M. sauron*, *M. schomburgkii*, *M. tiete*, and *M. zorroi*).

For the new generated sequences, the samples were obtained from tissues stored in 95% ethanol and deposited at LBP tissue collection. The DNA extractions were made using the Promega DNA extraction kit, according to the manufacturer's instructions. The segments of the COI gene were amplified by Polymerase Chain Reaction (PCR), with the primers Fish F6/R7 described by Jennings *et al*. (2019). The PCR reaction volume was 12.5 ul, composed by 7.55 ul of ddH2O, 1.25 ul of PCR buffer, 0.50 ul of MgCl (50mM), 0.25 ul of primer Fish F6/R7 (5uM) each, 0,50 ul dNTPs (2mM), 0.20 ul PHT Taq DNA polymerase, and 2 ul of DNA. The PCR consisted of denaturation (3 min at 95°C) followed by 30 cycles of denaturation (30 sec at 95°C), primer hybridization (45 sec at 52°C), nucleotide extension (1 min at 68°C), and a final extension (7 min at 68°C). The PCR products were first verified using agarose gel 1%, and then purified using ExoSapIT1 (USB Corporation), according to the manufacturer's instructions. The purified products were sequenced utilizing Big Dye TM Terminator v 3.1 and precipitated according to the alcohol precipitation protocol (https://assets.thermofisher.com/TFS-Assets/LSG/manuals/cms_081527.pdf), the amplified fragments were loaded into an ABI 3500 Genetic Analyzer (Applied Biosystems), in the Instituto de Biotecnologia (IBTEC).

From the forward and reverse sequences of each sample, we obtained and edited the consensus sequence through the Geneious Pro 5.5® software (Kearse *et al*., 2012).

The consensus sequences were aligned by MUSCLE (Edgar, 2004). We utilized the software MEGA v. 11 to estimate the best substitution model, which was Tamura-Nei +G+I according to BIC (Bayesian Information Criterion) (value was 9146.704). The phylogenetic reconstruction was carried a Maximum likelihood (ML) in the software RAxML. The confidence level of the branches was evaluated using 1,000 bootstrap replications. The overall interspecific and intraspecific distances were estimated with 1.000 pseudoreplicates. The results obtained were utilized in the mPTP (Kapli *et al*., 2017) and ASAP (Assemble Species by Automatic Partitioning) (Puillandre, Brouillet, Achaz, 2020) species discovery methods, with parameters in default.

TABLE 1. Summary of new generated sequences used in the molecular analysis.

Species	Voucher	Tissue number	Locality (river/basin/city/state)	Coordinates
Myloplus levis	LBP 27079	98411	Rio Mutum, Paraguay, Barão de Melgaço, MT	16°19'41"S 55°49'55"W
Myloplus levis	LBP 30256	104967	Rio Quilombo, Paraguay, Chapada dos Guimarães, MT	15°01'15"S 55°44'16"W
Myloplus levis	LBP 12644	47119	Rio Cuiabá, Paraguay, Corumbá, MS	19°00'04"S 57°35'37"W
Myloplus levis	LBP 13406	55821	Rio Bigueirinho, Paraguay, Poconé, MT	17°47'33"S 57°33'26"W
Myloplus animacula	LBP 7857	36898	Lagoa da Boca Franca, Araguaia, Cocalinho, MT	S 13°19' W 50°37'
Myloplus animacula	LBP 19075	75602	Afluente rio Laranjeiras, Tocantins, Goianésia, GO	15°08'47"S 48°53'19"W
Myloplus tiete	LBP 31564	109406	Rio Paraná, Paraná, Ilha Solteira, SP	20°26'31"S 51°23'35"W
Myloplus tiete	LBP 31564.1	109101, 109402, 109404	Rio Paraná, Paraná, Ilha Solteira, SP	20°26'31"S 51°23'35"W
Myloplus tiete	LBP 17233	68861	Ribeirão Blumado, Paraná, anta Cruz de Goiás, GO	17°17'41"S 48°32'00"W
Myloplus tiete	LBP 32711	111427,111429	Rio Paraná, Paraná, Ilha Solteira, SP	20°34'51"S 51°31'41"W

Myloplus tiete	NUP 13453	NUP 13453	Paraná	22°42'02"S 53°08'27"W
Myloplus sp.	LBP 25561	93338, 93339	Rio Palma, Tocantins, Lavandeira, TO	12°36'13"S 47°52'18"W
Myloplus sp.	LBP 25319	96294, 96295	Rio da Prata, Tocantins Iaciara, GO	12°25'19"S 47°12'13"W
Myloplus sp.	LBP 25724	95542	Córrego Insula, Araguaia, Barra do Garças, MT	15°53'13"S 52°02'00"W

1.3 Results

1.3.1 Redescription of *Myloplus levis*

Myloplus levis (Eigenmann, McAtee, 1907)

(Figs. 1–7, Tab. 2)

Myleus levis Eigenmann, McAtee, 1907:142, plate XLII [original description; type: N.10156, "Bahia Negra"] [currently type number: CAS 62107]. —Eigenmann, 1908:36 [listed; locality: Paraguay]. —Eigenmann, 1910:443 [listed]. —Sarmiento *et al*., 2014:187 [listed; reported from Bolivia]

Myloplus levis. —Eigenmann, 1914–1915:271–272 [new combination; listed; complementary description]. —Norman, 1929:825 [complementary description of three specimens from Paraguay]. —Britski *et al*., 2007:79 —Polaz *et al.*, 2014:126 [listed]. —Andrade *et al*., 2016a:572 [cited]. —Andrade *et al*., 2016b:572 [cited]. —Koerber *et al*., 2017:22 [listed]. —Machado *et al*., 2018:5 [listed; phylogeny based on COI]. —Andrade *et al*., 2019:e190026[2] [cited]. —Ota *et al*., 2020:6,17 [cited]. —Mateussi *et al*., 2020:3,7 [listed; phylogeny based on UCEs]. —Ota *et al*. in Gimênes Junior, Rech, 2022:235 [brief description]. —Soares *et al*., 2023:1,4,5,8

[cited]. —Toledo-Piza *et al*., 2024:413 [listed].

Myleus tiete non (Eigenmann, Norris). —Gosline, 1951:42 [in part; first mentioned as a junior synonym of *Myloplus tiete* (Eigenmann, Norris, 1900)]. —Géry, Mahnert, Dlouhy, 1987:446–447; Fig.54 [erroneously identified; cited as a junior synonym of *Myleus tiete*]. —Jégu in Reis, 2003:185 [listed as junior synonym of *M. tiete*]. - —Almirón *et al*., 2015:7,23,36,78 [erroneously identified; picture of color in life]

Myloplus cf. *asterias.* —Menni 2004:60; Fig.4.26 [erroneously identified; reported from Formosa, Argentina].

FIGURE 1. *Myloplus levis*, MZUSP 25277, female, 145.8 mm SL, Brazil, Mato Grosso, Itiquira municipality, rio Piquiri, Fazenda Santo Antônio do Paraíso.

Diagnosis. *Myloplus levis* can be diagnosed from all congeners by presenting serrae composed by long and slender spines (*vs*. short, with large base). The species differs further from all congeners, except *M. animacula* and *M. rubripinnis*, by presenting a markedly dark pigmentation on the distal portion of the first anal-fin rays (*vs*. distal portion hyalin or with diffuse dark pigmentation); from *M. animacula*, by presenting 23–

27 dorsal-fin branched rays (*vs*. 19–21); from *M. rubripinnis*, by presenting 8–14 post-pelvic spines (*vs*. 6–8). *Myloplus levis* can be distinguished from *M. arnoldi*, *M. lobatus*, and *M. torquatus*, by the absence of a marked black band on the caudal-fin distal margin (*vs*. presence); from *M. aylan*, *M. lobatus*, *M. sauron*, and *M. schomburgkii*, by the premaxillary teeth arranged in two juxtaposed rows (*vs*. two rows separated by internal gap forming a triangular space, in ventral view); from *M. aylan, M. sauron* and *M. schomburgkii*, by the absence of a vertical dark bar on the middle of the flank (*vs*. presence); from *M. nigrolineatus*, by never present pigmentation on the lateral line (*vs*. presence); and from *M. asterias*, by the rounded body (*vs*. elongated), and by the absence of marks on the flank (*vs*. scattered blotches of different colors and sizes, mainly during bleeding period). *Myloplus levis* differs from *M. tiete* by presenting longer dorsal-fin base [36.0–39.6% SL (mean 37.4) *vs*. 30.6–36.9% SL (mean 33.9); Fig. 2], shorter adipose-fin base (1.9–3.7% SL *vs*. 4.1–5.8% SL); shorter dorsal-fin end to anal-fin end distance [17.5–20.4% SL (mean 18.9) *vs*. 19.8–25.2% SL (mean 23.2); Fig. 2]; last unbranched ray of anal fin longer and thicker (*vs*. shorter and thinner); frontal fontanelle wide (*vs*. narrow) and predorsal spine short (*vs*. long).

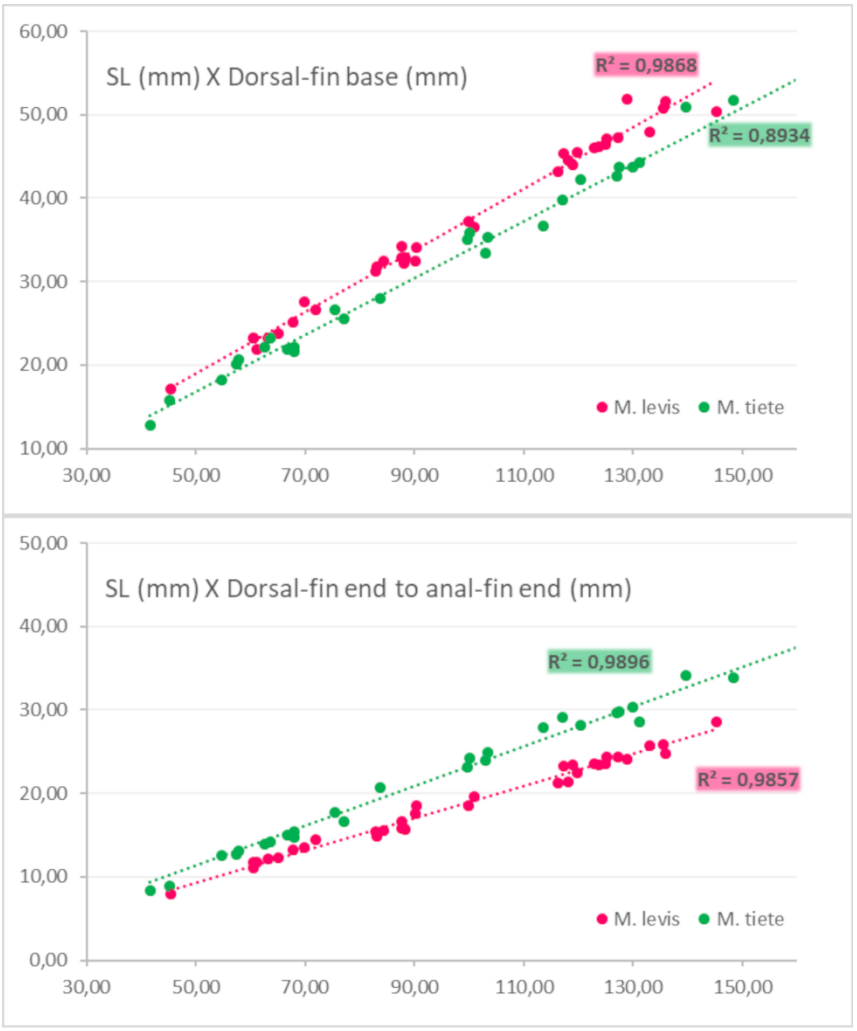

FIGURE 2. Regression analysis of some morphometric characters that help diagnose between *Myloplus levis* and *M. tiete*.

Description. Morphometric data presented in Tab. 2. Body compressed, rounded, with similar length and depth. Highest body depth at dorsal-fin origin. Predorsal and post-dorsal length almost similar. Head rounded, pre orbital distance slightly shorter than postorbital distance. Dorsal profile of head convex from mouth to horizontal through dorsalmost margin of the eye, and straight from this point to base of supraoccipital. Dorsal profile from the supraoccipital to the dorsal-fin insertion convex. Dorsal-fin base slightly convex. Dorsal profile straight from dorsal-fin base to adipose-fin base. Adipose-fin base straight, with distal margin about two times the base. Ventral profile of head and body convex from lower lip to the base of the first unbranched anal-fin ray. Anal-fin base straight. Dorsal and ventral profile of caudal peduncle concave.

Mouth terminal. Premaxillary teeth in two rows, outer row with 5(44) molariform teeth; teeth, 1–4 almost equal in size, tooth 5 smaller, all teeth with convex edges; inner row

with 2(5) equal-sized teeth with concave edges; all premaxillary teeth with sharp edges; in ventral view, contralateral outer rows forming convex arch; teeth 1 of contralateral outer rows not in contact at the symphysis; contralateral inner rows forming straight line between 3rd teeth of contralateral outer series; inner row in contact with outer row anteriorly. Dentary with 5(44) molariform teeth, teeth 1–3 substantially bigger than teeth 4–5. Conical symphyseal tooth immediately behind tooth 1 of labial row. Maxilla edentulous.

Scales small, cycloid. Perforated scales on lateral line 73(5), 74(1), 75(3), 76(1), 77(5), 78(4), 79(2), 80(3), 81(1), 82(2) or 83(1). Scale rows between dorsal-fin origin and lateral line 40(2), 42(4), 44(1), 46(2), 47(1), 48(3), 49(2), 50(1), 52(2), 53(2), 54(1), 55(1) or 56(2). Scale rows between lateral line and pelvic-fin origin 38(3), 39(3), 41(2), 42(1), 43(2), 44(2), 45(2), 46(3), 47(1), 48(1), 50(2), 53(1) or 55(1). Adipose-fin base covered by two or three scale rows. Scale rows between adipose-fin origin and lateral line 11(2), 12(2), 13(19), or 15(2). Circumpeduncular scales 30(5), 31(2), 32(1), 33(1), 34(2), 35(5), 36(1), 37(1), 38(2) or 39(2).

Dorsal-fin origin at vertical through pelvic-fin origin. Dorsal-fin rays iii, 23(1), 24(6), 25(14), 26(2) or 27(2). Adipose-fin trapezoidal, base shorter than distal extremities. Pectoral fin feather-shaped, anterior rays longest. Pectoral-fin rays i, 12(4), 13(5), 14(10), 15(7) or 16(1). Anterior pelvic-fin rays longest. Pelvic-fin rays i, 6(28). Last unbranched anal-fin ray most developed (longest and thickest). Anal-fin rays iii or iv, 31(2), 32(7), 33(14) or 34(5). Caudal fin forked, with approximately equal lobes. Gill rakers on first arch 10(1), 11(6) or 12(17) rakers on the upper branch; 1(24) on cartilage between cerato- and epibranchial; 12(5), 13(17), 14(1) or 15(1) on lower branch. Total gill rakers on first branchial arch 23(1), 24(4), 25(3), 26(14) 27(1) or 28(1).

Osteology. Dorsal profile of neurocranium convex from premaxilla to distal tip of its ascending process, straight at parietal, convex along supraoccipital process (Fig. 3). Supraoccipital process triangular in lateral view. Frontal fontanelle wide. Supraneurals 5(1) or 6(1). Dorsal-fin pterygiophores 26(1). First dorsal-fin pterygiophore inserted between neural spines of 10^{th} and 10^{th}(1) or 11^{th} and 12^{th}(1) vertebrae, with expanded anterior lamella and bearing forward-oriented short predorsal spine. Predorsal spine somewhat similar to scythe, dorsal surface smooth. Anal-fin pterygiophores 33(2). First anal-fin pterygiophore more developed, with anterior lamella.

Total vertebrae 40(1); Weberian apparatus 4(1); abdominal 19(1) [pre-dorsal, 8(1); under

dorsal fin 13(1)]; caudal 18(1) [under dorsal-fin 5(1); posterior to dorsal-fin 18(1)]. Insertion of anteriormost spine of ventral keel, anterior to vertical through pectoral-fin origin. Long spines, with an almost uniform width throughout its length, with piecing tips. First prepelvic spines covered by skin, less developed than postpelvic ones. Prepelvic spines 24(1), 25(4), 26(1), 27(6), 28(4), 29(3), 30(5), 31(2) or 33(1); post-pelvic spines 8(4), 9(11), 10(6), 11(6), 12(6) 13(1) or 14(1); and paired spines around anus 6(1), 7(3), 8(7), 9(10) or 10(6). Total ventral keel spines 42(1), 43(3), 44(5), 45(2), 46(3), 47(1), 48(3), 49(2), 50(2), 51(1), or 52(1).

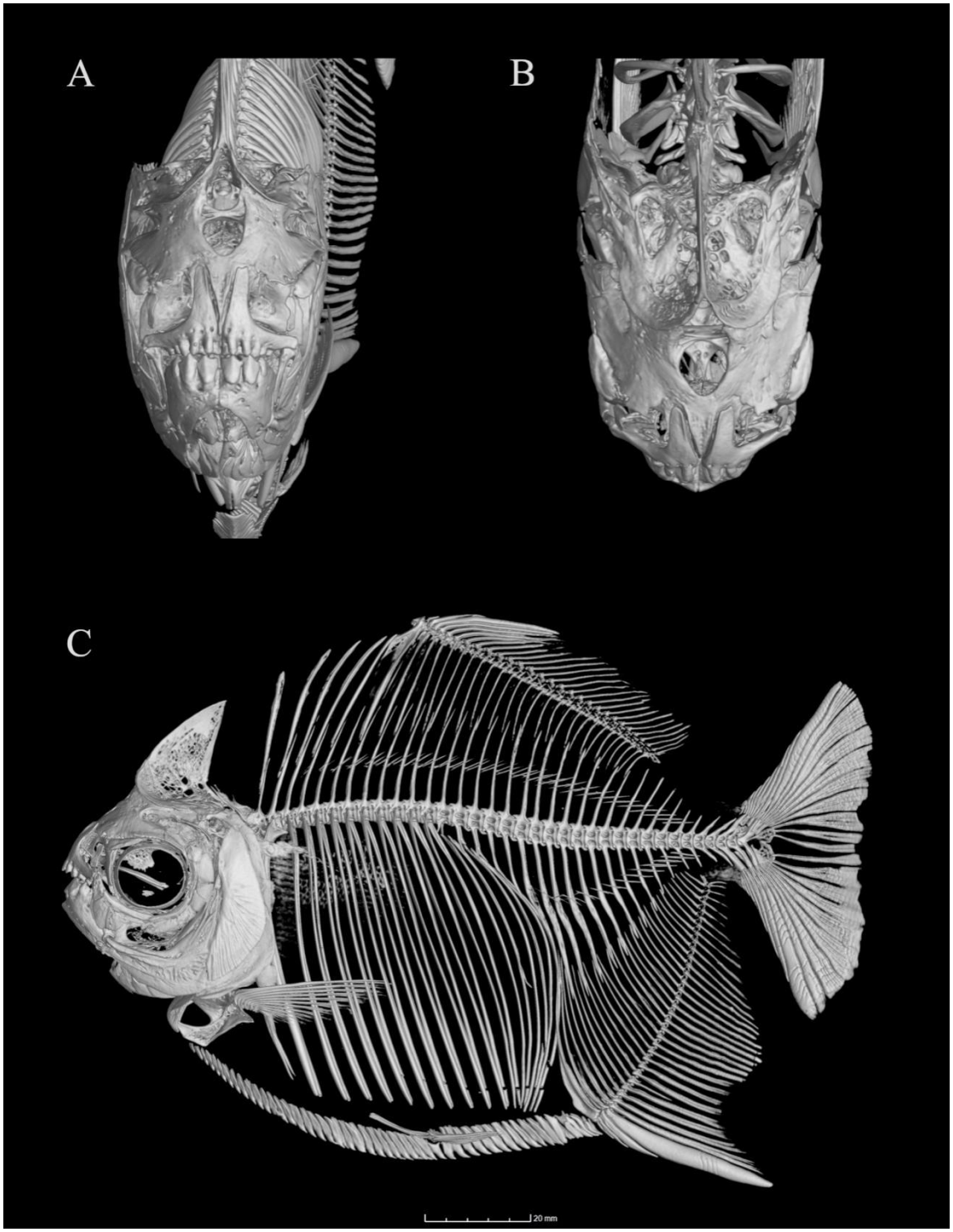

FIGURE 3. *Myloplus levis*, MZUSP 19810, male, tomography. **A.** Frontal view of head. **B.** Dorsal view of the head. **C.** Lateral view of the entire body.

TABLE 1. Morphometric data of *Myloplus levis*. SD= standard deviation. The highlighted lines are morphometric data that differentiates *M. levis* from *M. tiete*.

	Range	Mean	SD
Standard length (mm)	45.47–145.3		
		Percentages of SL	
Body depth	63.8–83.0	73.3	4.5
Head length	27.2–31.6	29.1	1.1
Supraoccipital process	11.8–21.3	16.6	2.0
Predorsal length	57.7–63.6	60.4	1.5
Postdorsal length	49.7–59.9	53.4	2.6
Prepectoral length	27.7–38.0	30.6	1.8
Prepelvic length	55.7–67.2	62.9	2.8
Preanal length	74.9–87.2	82.7	2.5
Dorsal-fin length	17.5–49.2	24.4	7.6
Interdorsal length	4.0–8.7	6.6	1.1
Pectoral-fin length	21.0–26.7	23.0	1.2
Pelvic-fin length	11.3–14.6	12.9	0.9
First anal-fin lobe length	21.9–50.4	28.5	5.1
Second anal-fin lobe length	11.8–16.3	13.3	2.2
Dorsal-fin base length	36.0–39.6	37.4	0.8
Adipose-fin base length	1.9–3.7	3.0	0.3
Anal-fin base length	35.9–47.4	40.8	3.1
Caudal-peduncle depth	8.4–9.8	9.3	0.4
Width of peduncle	2.6–4.9	3.6	0.5
Supraoccipital to dorsal-fin	38.6–50.3	45.8	2.0
Snout to Supraoccipital	14.8–44.8	30.3	5.7
Pelvic-anal distance	20.1–25.9	22.0	1.2
Pectoral-pelvic distance	25.8–39.2	32.6	2.6
Dorsal- to anal-fin origin	71.7–87.0	77.1	3.9
Dorsal-fin end to anal-fin origin	48.9–62.1	55.0	3.4
Dorsal- to end to anal-fin end	17.5–20.4	18.9	0.7
		Percentages of HL	
Width head	11.5–18.4	15.4	1.4
Postorbital distance	26.1–37.5	31.6	2.9
Fourth infraorbital width	9.3–15.9	12.0	1.4
Third infraorbital width	6.9–9.8	8.5	0.7
Cheek gap width	8.8–17.3	13.5	2.0
Interorbital width	38.9–62.2	52.8	4.9
Eye vertical diameter	27.1–41.2	33.7	2.8
Snout length	29.8–37.7	33.5	2.0
Mouth length	34.1–43.5	37.9	2.1
Mouth width	27.4–37.5	31.7	2.4
		Percentage of adipose-fin base length	
Adipose-fin length	0.4–1.0	0.7	0.1

Color in alcohol. Based on old and recently fixed specimens. Ground coloration brownish-olive or dark yellow dorsally to lateral line, fading to gray or light yellow ventrally. Head dark dorsally, vertical dark bar across eye, sclera light yellow. Paired fins hyaline, with light yellow tint. Dorsal and caudal fins translucent, with dark grey or a dark yellow hue. First rays of anal fin, until about the 13th branched ray, might present an orange pigmentation from the base to about two thirds of anal-fins rays' extension (present only in recently preserved specimens), becoming dark brown or black from this point until the distal tips (common in almost all fixed specimens) (Fig. 1).

Color in life. Ground coloration whitish silver. Iridescent bluish-green scales on dorsal region of body. Head dark anterodorsally, from upper lip to interorbital region; posteroventral portion of head whitish, with scattered yellow pigmentation. Paired fins hyaline with subtle yellow pigmentation. Dorsal and caudal fins hyaline, with dark brown hue. Anal fin overall hyaline. Basal two thirds of first anal-fin lobe red; distal third black. Flank without marks (Fig. 4).

FIGURE 4. Specimen of female of *Myloplus levis* recently captured at rio Cuiabá, Paraguay river basin.

Sexual dimorphism. Mature males with second anal-fin lobe centered on 14th or 15th branched ray, approximately twice as long as first lobe. Juveniles and females without second anal-fin lobe, but with long, falcate first lobe. Filaments extending dorsal-fin branched rays, and stiff hooks on distal-most lepidotrichia (common in males of some Myleinae) apparently absent.

Geographical distribution. *Myloplus levis* is widespread in the Paraguay River basin in Brazil (Fig. 5) and is also found in the lower Paraguay River basin in Argentina and Paraguay (Menni, 2004, fig. 4.26, as *M.* cf. *asterias*) and in the lower Paraná River basin in Argentina (Almirón *et al*., 2015, as *M. tiete*). A population with variation morphological features were observed in upper Paraguay River. See details in Morphological Variation Section.

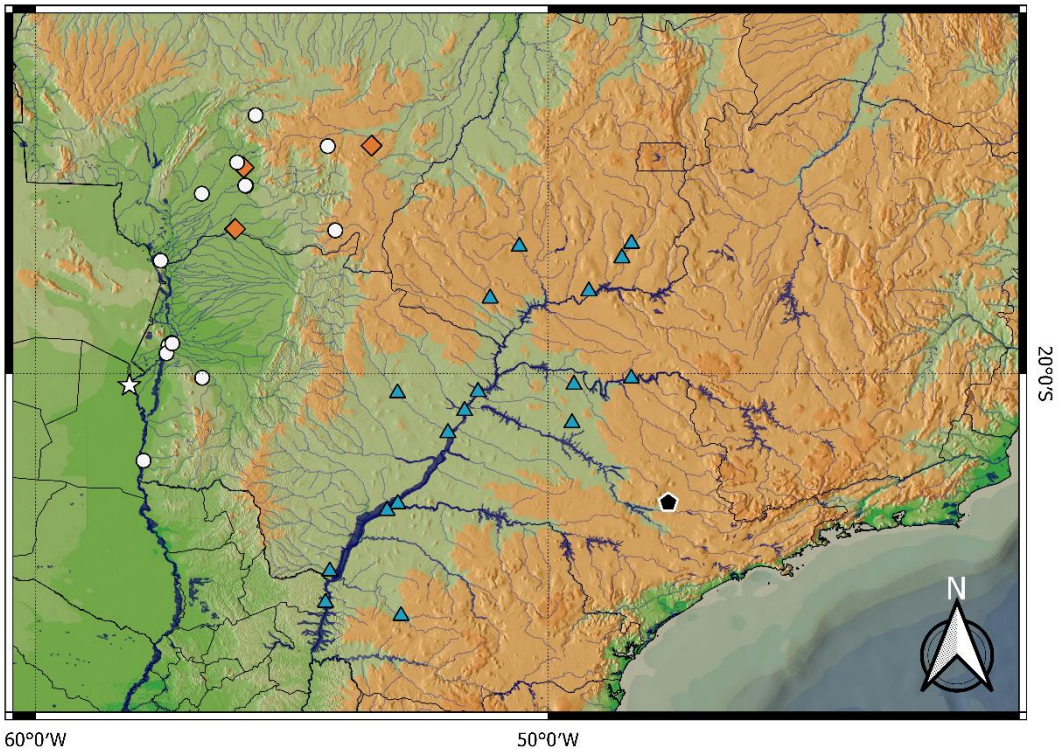

FIGURE 5. Map of South America Austral region showing geographic distribution of *M. levis* (white circles; white star, type locality), morphologically distinct specimens of *Myloplus levis* (orange diamond), and *Myloplus tiete* (blue triangles; black hexagon, type locality).

Remarks. Taxonomic history. *Myleus levis* was described based on a specimen from "Bahia Negra", in the Paraguay River basin (Eigenmann, McAtee, 1907). According to the authors, some of the holotype's characteristics are: "Length 143 mm; D. 27; A. 36; Ridge 45; Lateral line 112; conspicuous black spot on the margin of the anal fin, extending to the fourth or sixth ray". The specimen was originally deposited in the Indiana University (IU) collection and had the catalog number IU 10156 but is currently housed in the CAS (see taxonomic history of *M. tiete*), with the accession number CAS 62107 (Fig. 6).

Figure 6. *Myloplus levis*, holotype, CAS 62107.

More than four decades after its description, Gosline (1951) proposed that *M. levis* is a junior synonym of *M. tiete*. Although the species were described from different portions of the Paraná-Paraguay River basin, the author argued that Eigenmann did not provide a comparison between these species, thus no diagnostic characters between them was cited. The Gosline's hypothesis was followed by Géry (1976, 1977) and Géry *et al*. (1987) and was only opposed years later by Jégu (2003); however, at that time, Jégu also did not provide a diagnosis between *M. levis* and *M. tiete*. Since then, the species have been

recognized as distinct taxa, but due to the lack of a proper taxonomic review, they are identified mainly based on the basin in which they are caught.

Morphologic variation. According to the analysis of the specimens used in this study and based on illustrations or photos published in other works (see synonymic list), we can affirm that the majority of specimens identified as *Myloplus levis* present very distinctive morphological characteristics (*i.e*., a body as deep as long or deeper than long, absence of marks on the flank; and the tips of the first rays of the anal fin with strong dark pigmentation) (Fig. 7). However, three of the lots analyzed (MZUSP 52528; NUP 2159; ZUEC 6609) exhibit phenotypic characteristics different from those normally found in the species. These specimens have a body longer than deep and spots of various sizes and colors scattered on the body (very similar to those presented in *Myloplus asterias*). Although they present significant morphological differences, morphometric and meristic data are not yet substantial for proposing a new species. Furthermore, some of these specimens share the dark pigmentation on the tips of the first rays of the anal fin, which does not favor their identification as *M. asterias*. Ota *et al.* (in Gimênes Junior, Rech, 2022:235) analyzed material from the Pantanal, providing photos of the coloration in life of males and females, identified as *Myloplus levis*, which exhibit the marks scattered on the flank, in addition to the characteristic pigmentation on the anal fin of the species. Since few specimens analyzed herein have these characteristics and tissues for DNA extraction are unavailable, we tentatively point out this morphotype as a variation of *M. levis*.

FIGURE 7. Different morphotype of *Myloplus levis* with body longer than deep and spots of various sizes and colors scattered on the body, ZUEC 6609, male, 141.5 mm SL.

Material Examined. Non-type specimens. Brazil: Mato Grosso: LBP 9868, 2, 48.1–50.1 mm SL, Miranda municipality, rio Miranda, Paraguay basin, 19°47'05"S 56°49'19"W, 26 Nov 2009, C. Oliveira. LBP 12644, 1, (47119), 99.1 mm SL, Corumbá municipality, rio Cuiabá, Paraguay basin, 19°00'04"S 57°35'37"W, 24 Oct 2010, R. Britzke, L. R. Gaspar & B. F. Melo. LBP 13406, 1, (55821), 60.6 mm SL, Poconé municipality, rio Bigueirinho, tributary of rio Paraguay, 17°47'33"S 57°33'26"W, 28 Oct 2010, R. Britzke, L. R. Gaspar & B. F. Melo. LBP 27079, 1, (98411), 45.5 mm SL, Barão do Melgaço municipality, rio Mutum, tributary of rio Paraguay, 15 Mar 2018, N. Flausino Junior, N. Estevão & F. A. Machado. LBP 32738, 1, (111240), 79.8 mm SL, rio Manso, tributary of rio Paraguay, 14°52'22.24"S 55°47'52.93" W, 11 Feb 2022, A. Nobile. MZUSP 19795, 1, 114.0 mm SL, Poconé municipality, Campo do Jofre, 16°14'00"S 56°36'59", 10 Feb 1977, CEPIPAM. MZUSP 19842, 4, 82.9–90.3 mm SL, Barão do Melgaço municipality, rio Cuiabá, 16°11'38"S 55°58'05"W, 4 Oct 1977, CEPIPAM. MZUSP 25277, 4, 110.5–144.3 mm SL, Itiquira municipality, rio Piquiri, Fazenda Santo Antônio do Paraíso, 17°12'04"S 54°08'55"W, 24 Oct 1978, J. C. Oliveira. MZUP 52528, 1, 139.4 mm SL, rio Piquiri, pantanal de Paiaguás region, Baía da sede, Fazenda Santo

Antônio, 17°18'31"S 56°43'06"W, 18 Mar 1993, T. Lipparelli/Projeto Tucunaré-Piranha. NUP 1054, 1, 110.1 mm SL, Rosário Oeste municipality, Reservatório Manso, 14°41'49"S 56°14'31"W, 14 Nov 2003, Nupélia. NUP 2174, 1, 141.0 mm SL, Alto Garças municipality, Rio das Garças, 16°53'51"S 53°24'02"W, 17 Dez 2000, Nupélia. NUP 3011, 8, 116.1–127.2 mm SL, Alto Garças municipality, Rio das Garças, 16°46'24"S 53°24'32"W, 21 Nov 2003, Nupélia. NUP 3012, 8, 115.0–140.3 mm SL, Alto Garças municipality, Rio das Garças, 16°46'24"S 53°24'32"W, 21 Nov 2003, Nupélia. NUP 4142, 14, 103.4 mm SL, Alto Garças municipality, Rio das Garças, 16°42'57"S 53°24'39"W, 1 Set 2003, Nupélia. NUP 6366, 5, 60.6–67.8 mm SL, Rosário Oeste municipality, Reservatório Manso, 14°56'59"S 55°41'59"W, 1 Set 2003, Nupélia. ZUEC-PIS 4309, 4, 61.3–36.2 mm SL, Poconé municipality, rio Piraputanga, 16°15'53"S 56°40'33"W, 1 Apr 1999, F. A. Machado, I. Sazima & C. M. C. Leite. ZUEC 6609, 1, 142.6 mm SL, Cuiabá municipality, olho d'água perto da Serra de São Vicente, rio Cuiabá, 15°36'10"S 56°08'31"W, 1 Dez 2004, W. P. Troy. ZUEC 10041, 2, 78.6–99.8 mm SL, São José do rio Claro Municipality, rio Claro, acima da estrada MT-235, 13°51'24"S 56°41'11"W, I. M. Fernandes & G. M. Alencar. **Mato Grosso do Sul:** DZSJRP 5478, 1, 125.8 mm SL, Miranda municipality, rio Miranda, tributary of rio Paraguay, Morro do Azeite, Fazenda Bodoquena, 20°07'01"S 56°44'47"W, 1 Jan 1989, V. Garutti. DZSJRP 7801, 1, 145.3 mm SL, Miranda municipality, rio Miranda, Morro do Azeite, Fazenda Bodoquena, 20°07'01"S 56°44'47"W, 1 Nov 1989, V. Garutti. MNRJ 44721, 1, 139.6 mm SL, Corumbá municipality, rio Paraguai, imediatamente a jusante do local previsto para a construção do porto, 5 Set 2011, A. C. G. Pacheco & E. L. S. Peçanha. MNRJ 44882, 1, 80.3 mm SL, Corumbá municipality, ponto 1, a montante do local de construção da adutora do rio Paraguai, 8 Oct 2011, A. C. G. Pacheco & E. L. S. Peçanha. MZUSP 25281, 1, 153.77 mm SL rio Piquiri, fazenda Santo Antônio do Paraíso, município de Itiquira, 17°12'31"S 54°09'05"W, J.H. Botelho Medeiros. NUP 168, 1, 118.9 mm SL, Porto Murtinho municipality, Baía da Medalha, 19°24'46"S 57°19'54"W, 16 Sep 1993, A. A. Agostinho. NUP 9905, 1, 127.2 mm SL, Porto Murtinho municipality, Lagoa Criminosa, 21°41'30"S 57°53'32"W, 9 Nov 2009, Y. Rondon Suarez. NUP 12557, 2, 96.8–111.0 mm SL, Porto Murtinho municipality, Riacho Amonguijá, 21°41'09"S 57°52'53"W, 22 Mar 2010, Y. Rondon Suarez. NUP 13564, 3, 88.8–98.7 mm SL, Porto Murtinho municipality, Lagoa Albuquerque, 19°26'10"S 57°22'03"W, 27 Mar 2012, Nupélia. NUP 13625, 3, 88.0–99.8 mm SL, Porto Murtinho municipality, Baía do Bugre, 19°31'09"S 57°24'01"W, 25 Mar 2012, Nupélia. NUP 13636, 4, 119.8–128.9 mm SL,

Porto Murtinho municipality, Lagoa Figueirinha, 19°22'07"S 57°22'05"W, 27 Mar 2012, Nupélia. NUP 14351, 1, 121.2 mm SL, Porto Murtinho municipality, Lagoa Piúva, 19°26'47"S 57°23'09"W, 25 Mar 2012, Nupélia.

1.3.2 Redescription of *Myloplus tiete*

***Myloplus tiete* (Eigenmann, Norris, 1900)**
(Figs. 8–11; Tab. 3)

Myletes tieté Eigenmann, Norris, 1900:359–360 [spelling error; original description; type "um specimen de Piracicaba"; type locality: Piracicaba (=Brazil, São Paulo State)].

Myleus tiete Eigenmann, Kennedy, 1903:529–530 [new combination; additional description]. ―Eigenmann, 1910:443 [listed]. ―Gosline, 1951:42–43 [brief commentary indicating *Myloplus levis* as a junior synonym]. ―Géry, 1976:48–49 [listed]. ―Géry, 1977:262;263–265 [cited by the author as *M. tiete* from Paraguay basin; photo of a juvenile erroneously identified as *M. tiete* from Tocantins basin]. ―Gómez, Chebez, 1996:52 [cited from Argentina]. ―Jégu in Reis *et al*., 2003:186 [listed]. ―Sarmiento *et al*., 2014:187 [listed]. ―Mirande, Koerber, 2015:15 [listed]. ―Akama *et al*., 2018:62–64 [categorized as EN according to the IUCN criteria].

Myloplus tiete. ―Norman, 1929:826 [listed]. ―Jégu, 2001:386 [cited]. ―Ortí *et al*., 2008:348,350 [phylogeny based on mitochondrial DNA]. ―Andrade *et al*., 2016a:572,578 [cited]. ―Andrade *et al*., 2016b:572,578 [cited]. ―Koeber *et al*., 2017:2 [listed]. ―Andrade *et al.*, 2018:117 [cited]. ―Machado *et al*., 2018:5 [DNA barcode]. ―Jarduli *et al*., 2020:6,13 [listed]. ―Mirande, Koerber, 2019; 2020 [listed]. ―Andrade *et al*., 2019:e190026[2] [cited]. ―Reis *et al*., 2020:463 [listed]. ―Mateussi *et al*., 2020:3,7 [phylogeny based on UCEs]. ―Soares *et al*., 2023:5[cited]. ―Toledo-Piza *et al.*, 2024:415 [listed].

FIGURE 8. *Myloplus tiete*, female, LBP 31564, 237.2 mm SL, Ilha Solteira municipality, rio Paraná.

Diagnosis. Based on color features *Myloplus tiete* can be readily diagnosed from from *M. arnoldi*, *M. lobatus*, and *M. torquatus* by the absence of a marked black band on caudal-fin distal margin (*vs*. presence); from *M. aylan*, *M. sauron*, and *M. schomburgkii*, by the absence of a vertical bar on the middle of the flank (*vs*. presence); from *M. animacula*, *M. levis*, and *M. rubripinnis*, by the absence of markedly dark pigmentation on the first anal-fin rays (*vs.* presence); and from *M. asterias* and *M. nigrolineatus* by the absence of scattered blotches with different colors on the flank. Additionally, it differs from *M. nigrolineatus*, *M. tumukumak* and *M. zorroi* by having 60–84 perforated scales on the lateral line (*vs*. 89–114, 56–65 and 85–89, respectively); from *M. aylan*, *M. lobatus*, *M. sauron*, and *M. schomburgkii* by the premaxillary teeth arranged in two juxtaposed rows (*vs*. with internal gap forming a triangular space, in ventral view); and from *M. asterias*, *M. arnoldi*, *M. animacula*, and *M. levis* by having 40 vertebrae (*vs*. 37–38) The species differs from *M. lucienae* by presenting i, 6 pelvic-fin rays (*vs*. i,7), 40 vertebrae (*vs*. 41), and by higher number of pre-pelvic spines (26–31 *vs.* 15–23), and total spines (35–54 *vs.* 28–38). *Myloplus tiete* can be further distinguished from *M. levis* by a smaller dorsal-fin base [30.6–36.9% SL (mean 33.9) *vs*. 36.0–39.6% SL (mean 37.4) Fig. 2], longer adipose-fin base (4.1–5.8% SL *vs*. 1.9–3.7% SL); longer dorsal-fin end to anal-fin end distance

[19.8–25.2% SL (mean 23.2) *vs*. 17.5–20.4% SL (mean 18.9) Fig. 2]; serrae composed by short spines with wide bases (*vs*. long and with narrow bases); last unbranched anal-fin ray short and narrow (*vs*. long and thicker); frontal fontanelle narrow (*vs*. wide); and predorsal spine long (*vs*. Short, Fig. 2).

Description. Morphometric data presented in Table 3. Body compressed, oval, with highest body depth at dorsal-fin origin. Predorsal length slightly longer than postdorsal. Head rounded, eye almost at center of the head, pre-orbital distance slightly shorter than postorbital distance. Dorsal profile of head convex from the upper lip to the distal tip of premaxillae, and straight to slightly concave from this point to base of supraoccipital. Dorsal profile between supraoccipital base and dorsal-fin insertion convex. Dorsal-fin base slightly convex. Dorsal profile straight between dorsal and adipose fins. Adipose-fin base straight. Ventral profile of head and body convex from lower lip to the base of the last branched anal-fin ray. Anal-fin base convex. Dorsal and ventral profile of caudal peduncle concave.

Mouth terminal. Premaxillary teeth in two rows, outer row with 5(65) molariform teeth; teeth 1–4 almost equal in size, tooth 5 smaller, all with convex edges, in ventral view; inner row with 2(60) equal-sized teeth with concave edges, in ventral view; all premaxillary teeth with sharp edges; in ventral view, contralateral outer rows forming a convex arch; teeth 1 of the contralateral outer rows not in contact at the symphysis; contralateral inner rows forming straight line between 3rd teeth of contralateral outer series; inner row in contact with outer row anteriorly. Dentary with 5(65) molariform teeth; teeth 1–3 substantially larger than 4–5. Conical symphyseal tooth immediately behind tooth 1 of labial row. Maxilla edentulous.

Scales large, cycloid. Perforated scales on lateral line 68(3), 69(2), 70(4), 71(1), 72(6), 73(5), 74(7), 75(3), 76(7), 77(8), 78(6), 79(2), 80(7), 81(8), 82(1), or 84(2). Scale rows between dorsal-fin origin and lateral line 30(1), 31(1), 33(1), 34(5), 35(1), 36(5), 37(7), 38(4), 39(6), 40(1), 41(5), 42(5), 43(3), 44(1), 45(6), or 46(3). Scale rows between lateral line and pelvic-fin origin 30(1), 31(1), 32(2), 33(4), 35(6), 36(6), 37(3), 38(2), 39(3), 40(3), 41(2), 42(7), 43(2), or 44(2). Adipose-fin base covered by three or four scale rows. Scale rows between adipose-fin origin and lateral line 11(3), 12(2), 13(24), or 15(3). Circumpeduncular scales 28(2), 29(6), 30(8), 31(7), 32(7), 33(4), 34(2), 35(1), 36(4), or 37(1).

Dorsal-fin origin slightly anterior to vertical through pelvic-fin origin. Dorsal-fin rays ii-

iii, 21(1), 23(14), 24(15), 25(15), or 26(6). Adipose-fin rectangular, longer than high. Pectoral fin feather-shaped, anterior rays longest. Pectoral-fin rays i, 13(1), 14(3), 15(26) or 16(13). Anterior pelvic-fin rays longest. Pelvic-fin rays i, 6(41). Last unbranched anal-fin ray most developed (longest and thicker). Anal-fin rays iii or iv, 27(1), 29(1), 30(3), 31(12), 32(10), 33(14), 34(4) or 36(1). Caudal-fin forked, lobes approximately equal. Gill rakers on first arch 10(6), 11(5) or 12(13) on upper branch; 1(24) on cartilage between cerato- and epibranchial; and 11(2), 12(13), or 13(8) on lower branch. Total gill rakers on first branchial arch 23(5), 24(6), 25(6) or 26(6).

Osteology. Dorsal profile of neurocranium convex from premaxilla to distal tip of its ascending process, straight at parietal, convex along supraoccipital process (Fig. 9). Supraoccipital triangular in lateral view. Frontal fontanelle narrow, elongated. Supraneurals 7(2). Dorsal-fin pterygiophores 24(2). First dorsal-fin pterygiophore between neural spines of 12^{th} and 13^{th}(1) vertebrae, with expanded anterior lamella and bearing long, forward-oriented spine. Predorsal spine somewhat similar to scythe, dorsal surface smooth. Anal-fin pterygiophores 33(2). First anal-fin pterygiophore more developed, with anterior lamella.

Total vertebrae 41(1); Weberian apparatus 4(1); abdominal 19(1) [pre-dorsal, 8(1); under dorsal-fin 13(1)]; caudal 18(1) [under dorsal-fin 5(1); posterior to dosal-fin 18(1)]. Insertion of anteriormost spine of ventral keel anterior to vertical through pectoral-fin origin. Short spines, with base two times bigger than the tips (Fig. 9 c), with piercing tips. First prepelvic spines covered by skin, less developed than post-pelvic ones. Prepelvic spines 26(3), 27(2), 28(1), 29(4), 30(7) or 31(9); postpelvic spines 8(3), 9(10), 12(1), 13(1) or 14(1); paired spines around anus 5(2), 6(3), 7(6), 8(19), 9(7) or 10(1). Total ventral keel spines 36(1), 42(2), 43(2), 44(4), 45(2), 46(4), 47(3), 48(8), 49(4), 50(6), 51(1), 52(2), 53(1) or 54(1).

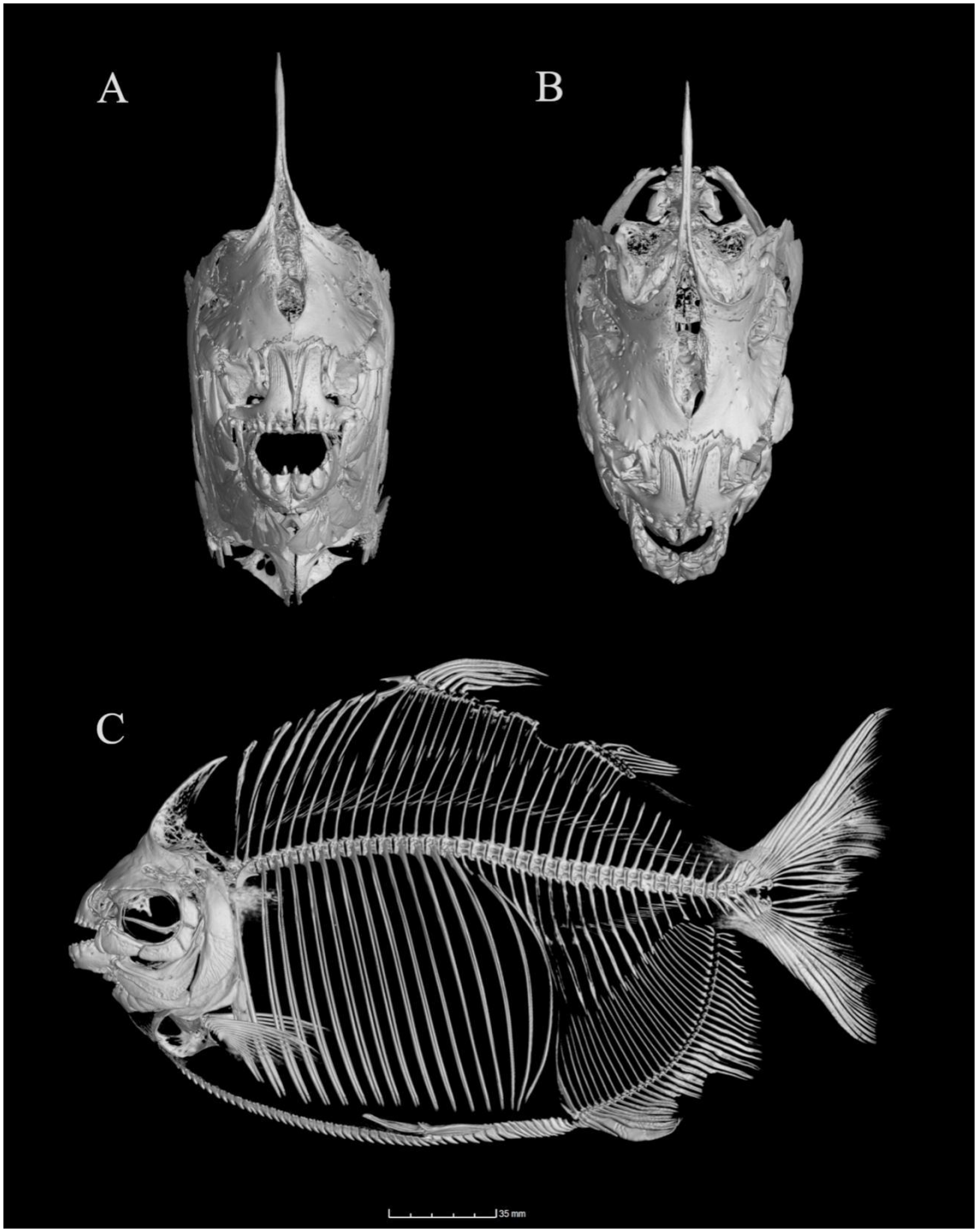

FIGURE 9. *Myloplus tiete*, MZUSP 12505, male, 168.3 mm SL, tomography. **A.** Frontal view of head. **B.** Dorsal view of the head. **C.** Lateral view of the entire body.

Table 3. Morphometric data of *Myloplus tiete*. SD= standard deviation. The highlighted lines are morphometric data that differentiates *M. tiete* from *M. levis*.

	Range	Mean	SD
Standard length (mm)	40.4–262.5	142.2	
		Percentages of SL	
Body depth	55.1–76.0	68.8	4.3
Head length	21.0–28.2	24.2	1.9
Supraoccipital process	11.3–32.5	15.0	3.2
Predorsal length	57.8–62.5	60.0	1.2
Postdorsal length	48.1–59.0	54.5	2.2
Prepectoral length	21.4–28.7	24.7	2.1
Prepelvic length	55.2–66.0	60.1	2.9
Preanal length	77.1–85.7	80.8	1.8
Dorsal-fin length	18.2–36.2	24.3	3.9
Interdorsal length	7.1–10.7	8.9	0.8
Pectoral-fin length	18.2–20.0	20.2	1.0
Pelvic-fin length	11.9–15.6	14.1	0.9
First anal-fin lobe length	12.7–30.5	20.0	4.0
Second anal-fin lobe length	10.6–15.5	12.9	1.6
Dorsal-fin base length	30.6–36.9	33.9	3.9
Adipose-fin base length	4.1–5.8	4.9	0.4
Anal-fin base length	32.6–40.6	36.8	2.4
Caudal-peduncle depth	9.0–11.7	10.1	0.6
Width of peduncle	2.3–4.6	3.3	0.5
Supraoccipital to dorsal-fin	39.0–49.5	44.4	2.3
Snout to Supraoccipital	13.0–45.5	31.0	5.0
Pelvic-anal distance	19.5–26.6	23.6	1.8
Pectoral-pelvic distance	29.4–39.6	35.4	1.9
Dorsal- to anal-fin origin	64.0–80.7	72.8	3.6
Dorsal-fin end to anal-fin origin	46.4–58.7	52.7	3.1
Dorsal- to end to anal-fin end	19.8–25.2	23.2	1.2
		Percentages of HL	
Width head	13.0–15.9	14.7	0.8
Postorbital distance	20.6–38.3	31.1	3.9
Fourth infraorbital width	10.2–19.6	13.0	1.7
Third infraorbital width	8.3–17.1	11.6	1.7
Cheek gap width	7.5–19.1	13.5	2.3
Interorbital width	33.3–57.7	48.7	5.1
Eye vertical diameter	22.3–42.1	30.5	4.1
Snout length	27.3–39.7	34.7	2.8
Mouth length	27.8–39.3	34.2	2.5
Mouth width	24.8–35.5	31.5	2.3
		Percentage of adipose-fin base length	
Adipose-fin length	0.9–1.8	1.3	0.2

Color in alcohol. Ground coloration brownish-gray dorsal to lateral line, yellow ventrally to it. Males might present scattered brown pigmentation, forming two irregular stripes, one above and one below lateral line; upper stripe from opercle to vertical through dorsal-fin insertion, arched dorsally; lower stripe from ventral portion of opercle, typically to anterior portion of anal fin, straight to ventrally arched. Fins hyaline, wish yellow tint. Pectoral fin with subtle dark pigmentation on the first rays. Juveniles exhibit several dark marks on flanks, ranging from vertically oval shapes to complete stripes with irregular formats (Fig. 10).

Figure 10. *Myloplus tiete*, NUP 13453, juvenile, 45.3 mm SL, Brazil, Mato Grosso do Sul, Taquarussu municipality, Rio Paraná.

Color in life. In specimens recently collected, ground coloration silver grayish, darker dorsally. Iridescent scales covering the whole flank, with green hue dorsally; whitish hue on belly, most concentrated on anteroventral portion of head and body; and rust gold hue above anal fin, variably conspicuous. Anterodorsal portion of head dark olive gray. Sclera light yellow. Males might present scattered dark chromatophores, forming an irregular horizontal band above and below lateral line; the upper band commonly starts from the

opercle and extends to the vertical through dorsal fin insertion, forming a somewhat convex band; the lower band commonly starts from the ventral portion of opercle and might extend to the anterior portion of anal fin, forming a somewhat straight to slightly convex band. Males and females occasionally with red to orange scattered pigmentation immediately next to opercle. Fins hyaline, with dark grey hue. First anal-fin rays slightly red, with thin line of black pigmentation on their margins. Light yellow pigmentation from base to middle portion of caudal fin.

Sexual dimorphism. Juveniles and females with anterior rays of anal fin forming long, falcate lobe. Mature males with extended middle anal-fin rays, forming second lobe centered on 15th or 16th branched ray, approximately twice as long as first lobe. Filaments extending dorsal-fin branched rays, and stiff hooks on distal-most lepidotrichia (common in males of some Myleinae) apparently absent (Fig. 11).

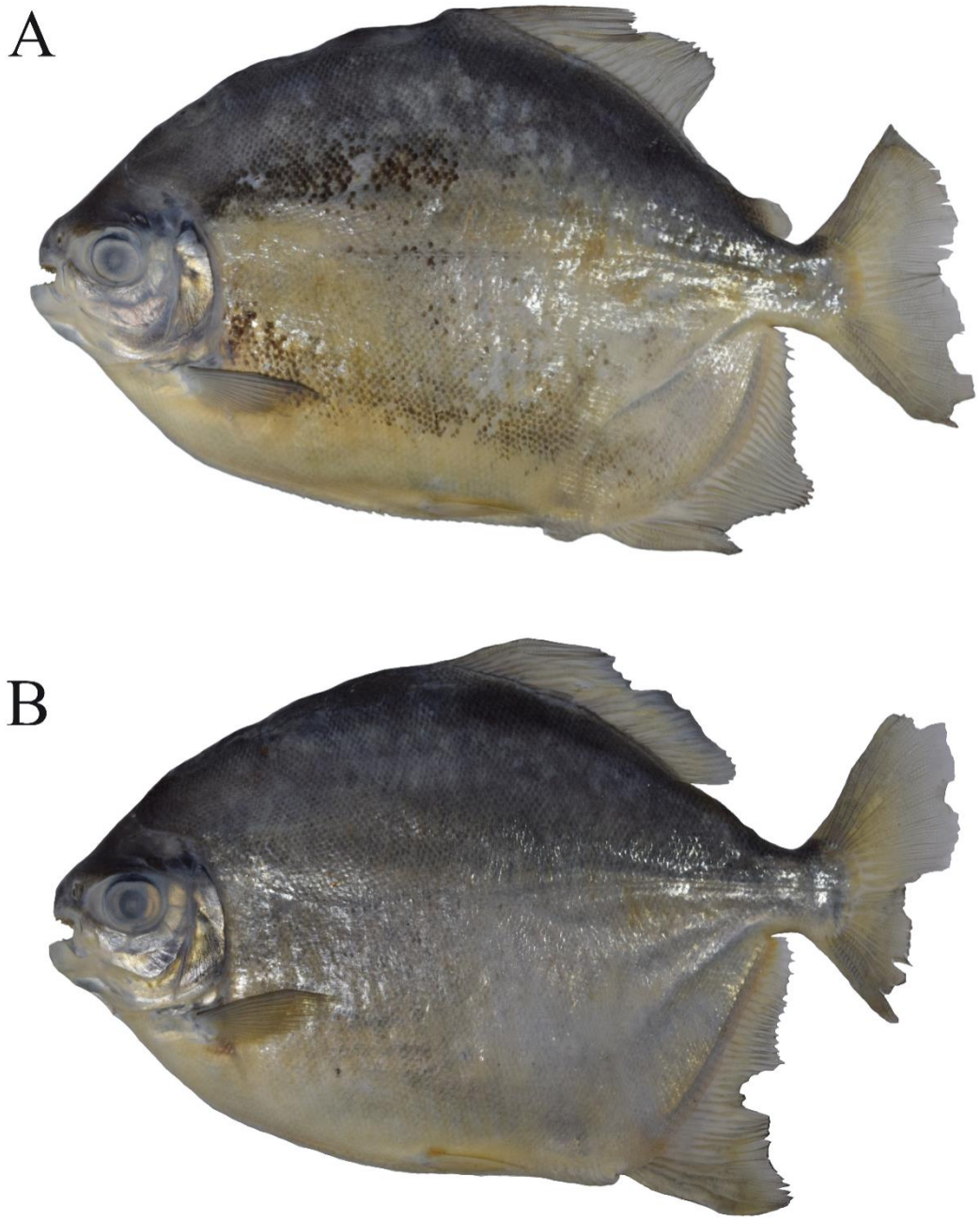

FIGURE 11. *Myloplus tiete*, LBP 31564 (109401, 109404). **A**. Male, 256.1 mm SL, with second lobe well developed. **B.** Female 235.3 mm SL. Both from Ilha Solteira municipality, rio Paraná.

Geographical distribution. *Myloplus tiete* is widespread in the upper Paraná River basin in Brazil (Fig. 5), including all its major tributaries, except the Ivaí River (see Reis *et al*., 2020).

Remarks. Taxonomic history. In 1900, Eigenmann and Norris analyzed specimens from the Paraná River basin deposited in the collection of Dr. H. von Ihering, at the Museu Paulista. Based on one of these specimens, they described *Myletes tieté = Myloplus tiete*, providing some characteristics regarding counts and color pattern (*e.g*. "D. i, 26; A. ii, 35; Serra 46; irregularly shaped vertical bands scattered over the flank that become spots below the lateral line; first five rays of the anal fin with dark brown coloration, followed by another five rays with bases pigmented in the same shade"), but they did not specify a type specimen, only indicating that it was "a specimen from Piracicaba", without detailed information.

Three years later, in 1903, Eigenmann and Kennedy published a work based on specimens from the Paraguay River basin. Although they were analyzing material from a different basin, Eigenmann took this opportunity to provide a complementary description of *Myleus tiete = Myloplus tiete*. In this description, the author mentions that "A specimen of this species was overlooked when the Reports on the fishes of São Paulo was prepared... The type was but 30 mm; the present specimen... 155 mm." (Fig. S3). The information provided matches that of the original description, except for the color pattern; the larger specimen does not have spots on the flanks; now we know that the color partner described for Eigenmann, Norris (1900), correspond to juvenile specimens.

Although from its original description it is not possible to pinpoint the specimen on which Eigenmann, Norris (1900) based the description of *Myloplus tiete*, based on the text, we can attest that the authors did so based on only one specimen, and therefore, this specimen is indeed the holotype of the species (see Art. 73.1.2. of ICZN, Machado *et al*., 2024, in press). Currently, according to Jégu in Reis (2003) and Fricke *et al*. (2024), the whereabouts of this specimen remain unknown. The specimens collected by H. von Ihering that were analyzed by Eigenmann, Norris (1900) were originally deposited in the IU (Indiana University) collection; however, these lots are currently housed at the CAS. A search of the CAS database reveals the existence of a lot of *Myloplus tiete*, previously deposited in IU, collected by H. von Ihering in Piracicaba, Brazil (CAS 12024, ex IU 10119). Considering only the few pieces of information provided in the original description, it would be possible for this to represent the holotype of *M. tiete*. However, through the analysis of the photograph of specimen CAS 10224 (Fig. S2), we can affirm that the specimen is about 150.0 mm SL; thus, based on Eigenmann's complementary description in Eigenmann and Kennedy (1903), this

specimen could not represent the holotype (see Taxonomic history) but rather could represent the specimen on which the author based the redescription. Detailed analyses of the specimen may help confirm this hypothesis. No other clues regarding the location of the holotype were found.

Material examined. Non-type. Goiás: DZSJRP 15584, 1, 171.9 mm SL, Caçu municipality, rio Claro, tributary of rio Paranaíba, upper Paraná Basin, 18°33'13"S 51°07'37"W, 1 Oct 2009, D. M. Rosa. DZJRP 16032, 7, 41.3–54.8 mm SL, Santo Antônio da Marra municipality, rio Verdão, tributary of rio Paranaíba, 17°32'30"S 50°33'30"W, 9 Jun 2012, S. Britto. LBP 17233, 1, 165.7 mm SL, Santa Cruz de Goiás municipality, Ribeirão Brumado, tributary of rio Paraná, 17°17'41"S 48°32'00"W, 26 Nov 2012, R. Devidé, B Melo, J. H.M. Martinez & G. S. C. Silva. NUP 1218, 2, 52.3–68.0 mm SL, Caldas Novas municipality, rio Corumbá, 17°45'51"S 48°33'26"W, 9 Apr 1999, Nupélia. NUP 1230, 16, 120.0–237.2 mm SL. Caldas Novas municipality, Reservatório Corumbá, 17°45'51"S 48°33'26"W, 9 Apr 1999, Nupélia. NUP 1341, 4, 130.0–211.1 mm SL, Caldas Novas municipality, Rio Corumbá, 17°29'01"S 48°22'12"W, 10 Set 1996, Nupélia. **Mato Grosso do Sul:** NUP 287, 1, 85.7 mm SL, Mundo Novo municipality, rio Iguatemi, 23°53'09"S 54°15'26"W, 29 Mar 1989, Nupélia. NUP 291, 1, 117.2 mm SL, Campo Novo do Parecis municipality, rio Verde, 21°10'52"S 51°57'05"W, 23 Jan 1993, Nupélia. **Minas Gerais:** DZSJRP 21398, 1, 45.2 mm SL, Conceição das Alagoas municipality, Córrego das Alagoas, 19°58'12"S 48°23'04"W50, 28 Jan 2012, D. Ribeiro. **Paraná:** MZUSP 43873, 1, 139.6 mm SL, Formosa do Oeste municipality, rio Piquiri (apertado), tributary of rio Paraná, divisa de Mariluz, 24°11'05"S 53°14'48"W, 22 Jan 1988, Nupélia. NUP 288, 2, 68.2–78.8 mm SL, Campina Da Lagoa municipality, rio Cantu, 24°44'58"S 52°51'37"W, 26 Apr 1989, Nupélia. MZUSP, 8, 131.1–205.8 mm SL, Campina da Lagoa municipality, rio Cantú (foz), tributary of rio Piquiri, rio Paraná, divisa Altamira do Paraná e Guaraniaçu, 24°45'28"S 52°51'31"W, 19 Jul 1988, H. Britski, Pavanelli & Deitós. **São Paulo:** DZSRJP 4554, 1, 113.8 mm SL, Rosana municipality, tributary of rio Paranapanema, 22°34'02"S 52°55'32"W, 1 Jan 1992, CESP de Salto Grand. DZSJRP 4825, 1, 127.5 mm SL, São Paulo municipality, Córrego da Rosana, tributary of rio Paranapanema, 22°34'02"S 52°55'32"W, 1 Jan 1992, CESP de Salto Grande. DZSRJP 4826, 1, 120.5 mm SL, Rosana municipality, Paranapanema drainage, 22°34'02"S 52°55'32"31W, 1 Jan 1992, CESP de Salto Grande. DZSRJP 20447, 1, 222.3 mm SL, São Paulo municipality, rio Paraná, jusante UHE Jupiá, 20°23'26"S 51°21'51"W, 1 Jan

1990, Polícia Ambiental Birigui. DZSRJP 20938, 6, 237.5–197.4 mm SL. LBP 4816, 1, 149.5 mm SL, Salto Grande municipality, rio Paranapanema, tributary of rio Paraná, 22°54'07"S 49°58'46"W, 1 Mar 2006, H. Brandão, A. P. Vidotto & V. Gomes. LBP 9188 (68861), 2, Chavantes municipality, rio Paranapanema, 23°07'48"S 49°42'03"W, 25 Jan 2006, A. P. Vidotto, H. Brandão, I. P. Ramos, J. C. dos Santos & E. D. Carvalho. LBP 31564, 13, (109401–109412) 172.5–220.3 mm SL, Ilha Solteira municipality, rio Paraná, 20°26'31"S 51°23'35"W, 24 May 2022, I. P. Ramos. LBP 32711, 1, (111427–11143), Rio Paraná, 23 Jun 2022, Instituto da Pesca.

1.3.3 Molecular data

The molecular dataset included 75 sequences with a median sequence length of 598 bp (range 389–638 bp). After the alignment and trimming, the length of the matrix was 642 bp, the frequency of nucleotides was A= 22.5%, C= 31.4%, G= 18.4%, T= 27.6%. *Myloplus tiete* is represented by 7 sequences, five of which are newly generated, while *M. levis* is represented by 4 sequences (Fig. 13), all newly generated. The distance between these lineages is 8.5%. In addition, we generated sequences of two specimens [LBP 7857 (36898), LBP 19075 (75602)] from Araguaia River basin that we morphologically identified as *M. animacula*. The analyses suggested that *M. levis* and *M. animacula* are sister taxa, with 3.5% of distance between them. Further, *Myloplus animacula* was recovered nested with "*Myloplus asterias* (Tocantins)" from Machado *et al.* (2018). We also detected a clade, *Myloplus* sp. "Tocantins" [all from LBP: 25319(96295); 25561(93338, 93339); 25724(95542)] that do not match with any other species sampled and might represent an undescribed species (Fig. 13). From the ASAP species delimitation method, we include the first and second partitions with the highest scores. ASAP1 and ASAP2 partitioned the dataset into 24 and 25 lineages, respectively. Both analyses recovered *Myloplus tiete* and *M. levis* as distinct lineages. mPTP delimitation method estimated the number of species between 19 and 39, also recovering *Myloplus tiete* and *M. levis* as distinct lineages.

FIGURE 12. *Myloplus levis*, LBP 12644(47119), female, 99.1 mm SL, Brazil, Corumbá municipality, rio Cuiabá, Paraguay basin.

1.4 Discussion

Myloplus tiete and *M. levis* are two species from the Paraguay-Paraná River basin that are commonly misidentified (see under taxonomic history of both species) (*e.g*. Ortega, Vari 1986; Menni, 2004; Almirón *et al*., 2015; Machado *et al*., 2018; Mateussi *et al*., 2020). Surprisingly, our results indicate that the two species are distinguished by multiple features and are easily recognizable by morphological characteristics, with at least 16 morphometric characters that can be used to separate them (see under diagnosis and morphological description). Using a morphological approach, we selected specimens that matched the diagnostic features of each species and conducted a molecular species delimitation using COI. The molecular analyses corroborated the morphological results, revealing an 8.5% genetic distance between them.

Thus, *Myloplus levis* was misidentified in two recently published phylogenetic studies (Machado *et al*., 2018; Mateussi *et al*., 2020), leading to the misguided conclusion that it is closely related to *M. tiete* or even identical to it. Thanks to these authors' contribution,

we had access to tissue samples used by Machado *et al*. (2018), and pictures (Fig. S3) from the *M. levis* voucher specimen utilized by Mateussi *et al*. (2020). The three samples used by Machado *et al.* (2018) (one identified as *Myloplus tiete* and two identified as *Myloplus levis*) were resequenced in order to verify its position in our DNA barcoding tree and compare our sequences to those already generated by the authors. In our studied the six sequences were recovered together with specimens of *Myloplus tiete*, which were distant from the clade identified by us as *Myloplus levis*. Although we did not sequence the sample used by Mateussi *et al*. (2020), the analysis of photography Fig. S4 revealed that it was a specimen of *M. tiete*. Thus, it is possible to affirm that *M. levis* had not been sampled for molecular analysis prior to the present work. *Myloplus levis* was recovered as sister taxon of *M. animacula*, and it is more related to Amazonian representatives of *M. asterias* than to *M. tiete*. In turn, *Myloplus tiete* appears as sister group of *M.* aff. *rubripinnis* from the Negro River basin.

The uncertainty between these taxa may had consequences beyond the field of taxonomy. Akama *et al*. (2018) considered *Myloplus tiete* as Endangered (EN) according to the criteria of the International Union for the Conservation of Nature. They based that decision on the observation that the records of *M. tiete* from most of its original geographic range have declined in the last decades. Deterioration of habitat conditions, mainly by the increasing number of dams like Itaipu, is likely the main reason for the population decreases. More recently, fishermen have reported the capture of many individuals of *M. tiete* at the Ilha Solteira Reservoir, which elicited a public demand to lift the restriction on its exploitation as food (personal communication).

Although we lack proper population studies for *Myloplus tiete*, by the analysis of specimens preserved in museums, it is possible to infer that: (1) preserved specimens from some of the main tributaries of the upper Paraná River basin, such as the Tiete, are rare; (2) most of the specimens analyzed herein were collected before 2014; (3) the species known distribution is restricted to the upper Paraná River Basin, and all of its reports from other basins, such as the Paraguay basin, are misidentifications. Even though the first and second inferences might be due to deficient sampling, by delineating its geographic distribution and providing a comprehensive diagnosis of the species, we enable populational studies that can generate more effective conservational strategies.

Myloplus tiete and *M. levis* are not isolated instances within the genus. As previously discussed, *Myloplus*, along with the majority of genera within Myleinae, is considered polyphyletic, contributing to our limited understanding of both inter- and

intra-generic relationships. The adoption of integrative taxonomy has played a crucial role in unveiling cryptic diversity within the group, facilitating the identification of novel species such as *M. nigrolineatus*, *M. aylan*, and *M. sauron*. Furthermore, it has proved invaluable in resolving longstanding taxonomic problems, as notably distinguishing between *M. tiete* and *M. levis*.

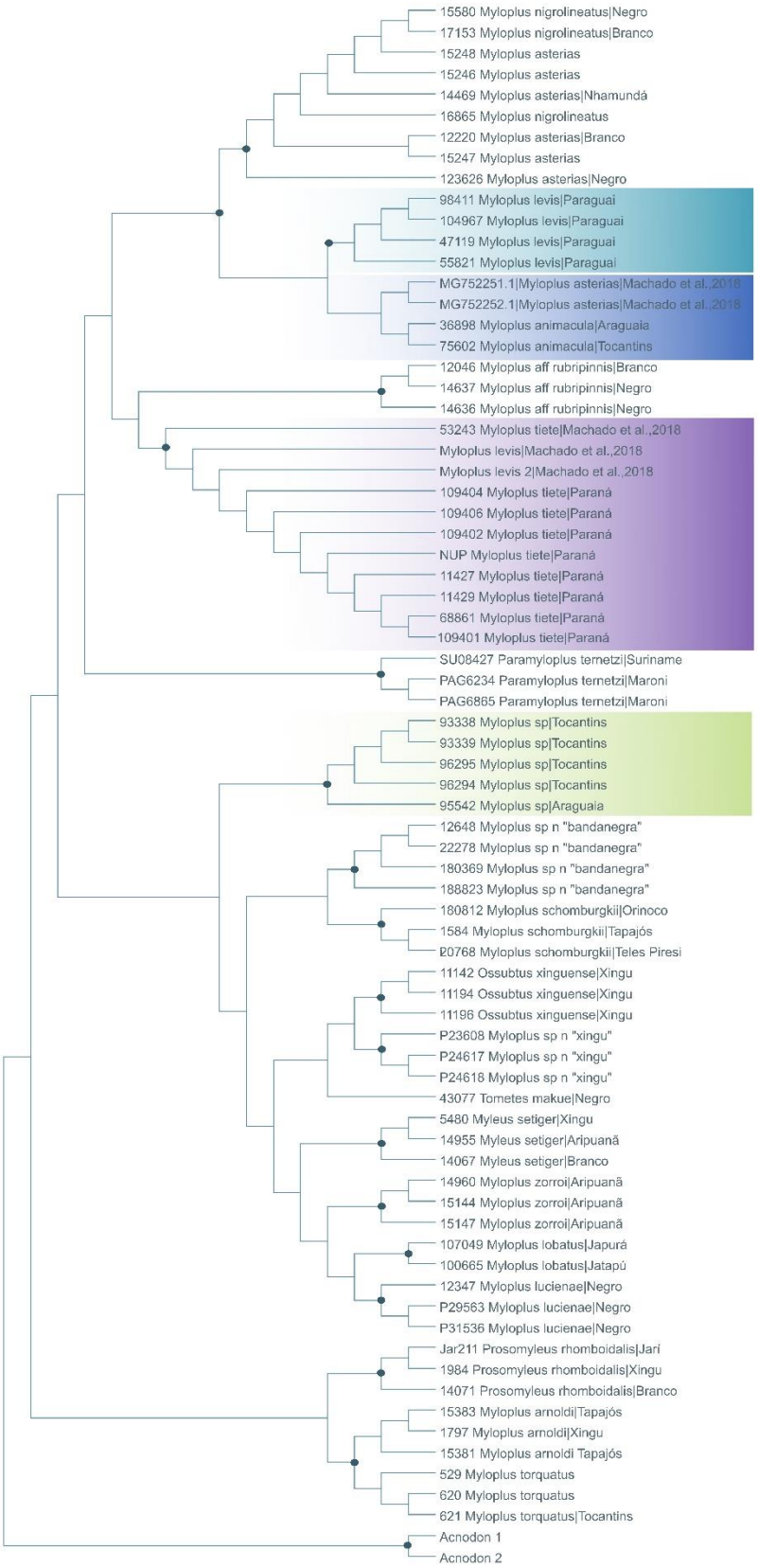

FIGURE 13. Maximum likelihood tree of species of the group Myleinae *sensu* Kolmann *et al.* (2020), based on the COI gene. Bootstrap values of 100% are represented by the dark nodes.

1.5 Comparative material.

Those given in Ota *et al*. (2020. Brazil: *Myleus gurupyensis*: NMW 10589, 175.0 mm SL, syntype. *Myloplus arnoldi*: INPA 45784, 4, 103.3-112.1 mm SL. *Myloplus asterias*: INPA 26871, 1, 156.0 mm SL; INPA 39331, 1, 171.9 mm SL; ZUFMS 4484, 2, 117.8-107.4 mm SL. *Myloplus lobatus*: INPA 53725, 208.2 mm SL. *Myloplus lucienae*: INPA 54771, 1, 167.6 mm SL. *Prosomyleus rhomboidalis*: INPA 40276, 2, 60.8-100.4 mm SL. *Myloplus rubripinnis*: INPA 4549, 2, 156.0-164.2 mm SL; INPA 53087, 2, 141.5-148.2 mm SL. *Myloplus schomburgkii*: INPA 30716, 1, 143.6 mm SL; ZUFMS 3703, 1, 122 mm SL. *Myloplus torquatus*: INPA 767, 148.1 mm SL; INPA 20013, 2, 68.2-90.1 mm SL; INPA 36702, 1, 77.5 mm SL. *Myloplus zorroi*: INPA 50880, holotype, 1, 326.2 mm SL. *Tometes maculatus*: MZUSP 3356, holotype, 168.3 mm SL. *Myleus planquettei*: French Guiana: INPA 2260, 90.9 mm SL. *Myloplus ternetzi*: INPA 3037, 2, 77.7-84.0 mm SL.

1.6 References

Akama A, Netto-Ferreira AL, Zanata AM, Calegari BB, Figueiredo CAA, Alves CBM, *et al*. *Myleus tiete* (Eigenmann, Norris, 1900). In: Instituto Chico Mendes de Conservação da Biodiversidade, organizer. Livro Vermelho da Fauna Brasileira Ameaçada de Extinção: Volume VI - Peixes. Brasília: ICMBio; 2018. p.228–30.

Almirón A, Casciotta J, Ciotek L, Giorgis P. Guía de los peces del Parque Nacional Pre-Delta. 2 ed. Buenos Ayres: Editorial APN; 2015.

Andrade MC, Jégu M, Buckup PA, Netto-Ferreira AL. A new *Myleus* species (Characiformes: Serrasalmidae) from the rio Tapajós basin, Brazil. J Fish Biol. 2018a; 92(6):1902–14. https://doi.org/10.1111/jfb.13628

Andrade MC, Jégu M, Giarrizzo T. *Tometes kranponhah* and *Tometes ancylorhynchus* (Characiformes: Serrasalmidae), two new phytophagous serrasalmids, and the first *Tometes* species described from the Brazilian Shield. J Fish Biol. 2016a; 89(1):467–94. https://doi:10.1111/jfb.12868

Andrade MC, Jégu M, Giarrizzo T. A new large species of *Myloplus* (Characiformes, Serrasalmidae) from the rio Madeira basin, Brazil. Zookeys. 2016b; 571:153–67. https://doi.org/10.3897/zookeys.571.5983

Andrade MC, López-Fernández H, Liverpool EA. New *Myloplus* from Essequibo

River basin, Guyana, with discussion on the taxonomic status of *Myleus pacu* (Characiformes: Serrasalmidae). Neotrop Ichthyol. 2019; 17(4):e190026. https://doi.org.10.1590/1982-0224-20190026

Andrade MC, Machado VN, Jégu M, Farias IP, Giarrizzo T. A new species of *Tometes* Valenciennes 1850 (Characiformes: Serrasalmidae) from Tocantins-Araguaia River Basin based on integrative analysis of molecular and morphological data. PLoS ONE. 2017; 12(4):e0170053. https://doi.org/10.1371/journal.pone.0170053

Britski HA, Silimon KZS, Lopes B. Peixes do Pantanal. Manual de Identificação. Brasilia: Embrapa Informação Tecnológica. 2007.

Campos AA. Sôbre os caracídios do rio Mogi-Guaçu (Estado de São Paulo). Arq. Zool. 1945; 4(11):431–65.

Edgar RC. Muscle: A multiple sequence alignment method with reduced time and space complexity. BMC Bioinformatics. 2004; 5:113. https://doi.org/10.1186/1471-2105-5-113

Eigenmann CH. Catalogue of the fresh-water fishes of tropical and south temperate America. Reports of the Princeton University Expeditions to Patagonia 1896–1899. Zoology. Fishes Patagonia. 1910; 3(4):375–511. https://doi.org/10.5962/bhl.title.2097

Eigenmann CH. The freshwater fishes of British Guiana, including a study of the ecological grouping of species and the relation of the fauna of the plateau to that of the lowlands. Mem Carnegie Mus. 1912; 5(1):1–578.

Eigenmann CH. The Serrasalminae and Mylinae. Ann Carnegie Mus. 1915; 9(3–4):225–72.

Eigenmann CH, Kennedy CH. On a collection of fishes from Paraguay, with a synopsis of American genera of cichlids. 1903; 55:497–537.

Eigenmann CH, McAtee WL, Ward DP. On further collections of fishes from Paraguay. Ann Carnegie Mus. 1907; (4):110–157.

Eigenmann CH, Norris AA. Sobre alguns peixes de S. Paulo, Brazil. Revista Do Museu Paulista. 1900; (4):349–362.

Eigenmann CH, Ogle F. An annotated List of characin fishes in the United States National Museum and the Museum of Indiana University, with descriptions of new

species. Proc. U. S. Natl. Mus. 1908; 33:35–68.

Escobar MD, Ota RP, Machado-Allison A, Andrade-López J, Farias IP, Hrbek T. A new species of *Piaractus* (Characiformes: Serrasalmidae) from the Orinoco Basin with a redescription *of Piaractus brachypomus*. J Fish Biol. 2019; 95(2):411–27. https://doi.org/10.1111/jfb.13990

Fricke R, Eschmeyer WN, Fong JD. Eschmeyer's catalog of fishes: genera, specie by family/subfamily [Internet]. San Francisco: California Academy of Science; 2024.

Géry J. Poissons Characoïdes des Guyanes. I. Généralités. II. Famille des Serrasalmidae. Zool Verh. 1972. 122(1): 1–250. http://www.repository.naturalis.nl/record/317730%5Cnhttp://www.repository.naturalis.nl/document/149016

Géry J. Les Genres de Serrasalmidae (PISCES, CHARACOIDEI). Bull Zool Mus. 1976; 5(6):47–54.

Géry J. Characoids of the World. Neptune City, New Jersey: T.F.H. Publications; 1977.

Géry J. The Serrasalmidae (Pisces, Characoidei) from the Serra do Roncador, Mato Grosso, Brasil. Amazoniana. 1979; 6(4): 467-495.

Géry J, Mahnert V, Dlouhy C. Possions characoïdes non Characidae du Paraguay (Pisces, Ostariophysi). Revue Suisse Zool. 1987; 94(2):357–464.,3

Gill NT. Note on the fshes of the genus Characinus. Proc U S Natl Mus. 1896; 18(1058):213–215. https://doi.org/10.5479/si.00963801.18-1058.213

Gimênes Junior, H; Rech, R. Guia ilustrado dos peixes do Pantanal e entorno. Campo Grande: Julien Design. 2022.

Gómez SE, Chebez JC. Fishes of the province of Misiones. En Fauna Misionera. Catálogo de los vertebrado de la Pcia de Misiones (Argentina). 1996.

Gosline WA. Notes on the Characid fishes of the subfamily Serrasalminae. Proc Calif Acad Sci. 1951; 27(2):17–64.

Goulding M. The fishes and the forest: explorations in Amazonian natural history. Berkeley: University of California Press; 1980.

Jarduli L, Garcia D, Vidotto-Magnoni A *et al*. Fish fauna from the Paranapanema River basin, Brazil. Bio Neotrop. 2020; 20(1): e20180707. http://dx.doi.org/10.1590/1676-0611-BN-2018-0707

Jégu M, Santos GM. Mise au point à propos de *Serrasalmus spilopleura* Kner, 1858 et

réhabilitation de *S. maculatus* Kner, 1858 (Characidae: Serrsalminae). Cybium. 2001; 25(2):119–143. http://dx.doi.org/10.26028/cybium/2001-252-002

Jégu M. Subfamily Serrasalminae (Pacus and Piranhas). In: Reis RE, Kullander SO, Ferraris CJ, Jr., editors. Check list of the freshwater fishes of South and Central America. Porto Alegre: Edipucrs; 2003. p.182–96.

Jégu M, Hubert N, Belmont-Jegu E. Réhabilitation de *Myloplus asterias* (Müller & Troschel, 1844), espèce-type de *Myloplus* Gill, 1896 et validation du genre *Myloplus* Gill (Characidae: Serrasalminae). Cybium. 2004; 28(2):119–57. https://doi.org/10.26028/cybium/2004-282-005

Jennings WB, Ruschi PA, Ferraro G, Quijada CC, Silva-Malanski ACG, Prosdocimi F *et al*. Barcoding the Neotropical freshwater fish fauna using a new pair of universal COI primers with a discussion of primer dimers and M13 primer tails. Genome. 2019; 62(2):77–83. https://doi.org/10.1139/gen-2018-0145

Kapli P, Lutteropp S, Zhang J, Kobert K, Pavlidis P, Stamatakis A *et al*. Multi-rate Poisson tree processes for single-locus species delimitation under maximum likelihood and Markov chain Monte Carlo. Bioinformatics. 2017; 33(11):1630–38. https://doi.org/10.1093/bioinformatics/btx025

Kearse M, Moir R, Wilson A, Stones-Havas S, Cheung M, Sturrock S *et al*. Geneious Basic: an integrated and extendable desktop software platform for the organization and analysis of sequence data. Bioinformatics. 2012; 28(2):1647–49. https://doi.org/10.1093/bioinformatics/bts199

Koerber S, Litz TO, Mirande JM. CLOFFAR - update 3 - supplement to Checklist of the Freshwater Fishes of Argentina. Ichthyological Contributions of Peces Criollos. 55:1-11

Kolmann MA, Hughes LC, Hernandez LP, Arcila D, Betancur-R R, Sabaj MH *et al*. Phylogenomics of piranhas and pacus (Serrasalmidae) uncovers how dietary convergence and parallelism obfuscate traditional morphological taxonomy. Syst Biol. 2020; 70(3):576–92. https://doi.org/10.1093/sysbio/syaa065

Machado VN, Collins RA, Ota RP, Andrade MC, Farias IP, Hrbek T. One thousand DNA barcodes of piranhas and pacus reveal geographic structure and unrecognized diversity in the Amazon. Sci Rep. 2018; 8:8387. https://doi.org/10.1038/ s41598-018-26550-x

Mateussi NTB, Melo BF, Ota RP, Roxo FF, Ochoa LE, Foresti F *et al*. Phylogenomics of the Neotropical fish family Serrasalmidae with a novel

intrafamilial classification (Teleostei: Characiformes). Mol Phylogenet Evol. 2020; 153:106945. https://doi.org/10.1016/j.ympev.2020.106945

Mattox GMT, Britz R, Toledo-Piza M. Skeletal development and ossification sequence of the characiform *Salminus brasiliensis* (Ostariophysi: Characidae). Ichthyol Explor Freshw. 2014; 25(2):103–58.

Menni RC. Peces y ambientes en la Argentina continental. Monogr. Mus. Argentino Cienc. Nat. 2004; (5):1–316.

Mirande JM, Koerber S. Checklist of the freshwater fishes of Argentina. 2nd edition. (CLOFFAR-2). Icthyological contributions of Peces Criollos. 2020; 72:1–81.

Norman JR. The South American characid fishes of the subfamily Serrasalmoninae, with a revision of the genus *Serrasalmus* Lacepède. Proc Zool Soc London. 1929; 98(52):781–829.

Ortí G, Sivasundar A, Dietz K, Jégu M. Phylogeny of the Serrasalmidae (Characiformes) based on mitochondrial DNA sequences. Genet Mol Biol. 2008; 31(1):343–51. https://www.scielo.br/j/gmb/a/WQBqC6FyNFCmFPqwN8jmXXh/?format=pdf&lang=en

Ota RP, Machado VN, Andrade MC, Collins RA, Farias IP, Hrbek T. Integrative taxonomy reveals a new species of pacu (Characiformes: Serrasalmidae: *Myloplus*) from the Brazilian Amazon. Neotrop Ichthyol. 2020; 18(1):e190112. https://doi.org/10.1590/1982-0224-20190112

Papa Y, Le Bail P-Y, Covain R. Genetic landscape clustering of a large DNA barcoding data set reveals shared patterns of genetic divergence among freshwater fishes of the Maroni basin. Mol Ecol Resour. 2021; 21(6):2109–24. https://doi.org/10.1111/1755-0998.13402

Polaz CNM, Melo BF, Britske R, Resende EK, Machado FA, Lima JAF, Petrere Júnior M. Fishes from the Parque Nacional do Pantanal Matogrossense, upper Paraguai river basin, Brazil. Check List. 2014; 10(1):122-130. https://doi.org/10.15560/10.1.122

Puillandre N, Brouillet S, Achaz G. ASAP: assemble species by automatic partitioning. Mol Ecol Resour. 2020; 21(2):p609-620. https://doi.org/10.1111/1755-0998.13281

Reis RE, Albert JS, Di Dario F, Mincarone MM, Petry P, Rocha LA. Fish

biodiversity and conservation in South America. J Fish Biol. 2016; 89(1): 12–47. https://doi.org/10.1111/jfb.13016

Reis BR, Augusto F, Deprá GC, Ota RR, Weferson JG. Freshwater fishes from Paraná State, Brazil: an annotated list, with comments on biogeographic patterns, threats, and future perspectives. 2020; 4868(4): 451–494. https://doi.org/10.11646/zootaxa.4868.4.1

Soares AB, Andrade MC, Lucinda PHF. A new species of *Myloplus* Gill 1896 (Teleostei: Serrasalmidae) from the Rio Tocantins basin, Brazil. Ichthyol Explor Freshw. 2023. http://doi.org/10.23788/IEF-1191.

Tamura K, Stecher G, Kumar S. MEGA11: Molecular Evolutionary Genetics Analysis version 11. Mol Biol Evol 2021; 38(7):3022–27. https://doi.org/10.1093/molbev/msab120

Toledo-Piza M, Baena EG, Dagosta FCP, Menezes NA, Ândrade M, Benine RC, Bertaco VA, Birindelli JLO, Boden G, Buckup PA, Camelier P, Carvalho FR, Castro RMC, Chuctaya J, Decru E, Derijst E, Dillman CB, Ferreira KM, Merxem DG, Giovannetti V, Hirschmann A, Jégu M, Jerep FC, Langeani F, Lima FCT, Lucena CAS, Lucena ZMS, Malabarba LR, Malabarba MCSL, Marinho MMF, Mathubara K, Mattox GMT, Melo BF, Moelants T, Moreira CR, Musschoot T, Netto-Ferreira AL, Ota RP, Oyakawa OT, Pavanelli CS, Reis RE, Santos O, Serra JP, Silva GSC, Silva-Oliveira C, Souza-Lima R, Vari RP, Zanata AM. Checklist of the species of the Order Characiformes (Teleostei: Ostariophysi). Neotrop Ichthyol. 2024; 22(1):e230086. https://doi.org/10.1590/1982-0224-2023-0086

Thompson AW, Betancur-RR, López-Fernández H, Ortí G. A time-calibrated, multi-locus phylogeny of piranhas and pacus (Characiformes: Serrasalmidae) and a comparison of species tree methods. Mol Phylogenet Evol. 2014; 81:242–57. http://dx.doi.org/10.1016/j.ympev.2014.06.018

Figures

FIGURE 1. *Myloplus levis*, MZUSP 25277, female, 145.8 mm SL, Brazil, Mato Grosso, Itiquira municipality, rio Piquiri, Fazenda Santo Antônio do Paraíso.
FIGURE 2. *Myloplus levis*, MZUSP 19810, male, tomography. **A.** Frontal view of head. **B.** Dorsal view of the head. **C.** Lateral view of the entire body.

FIGURE 3. Geographic distribution of *Myloplus tiete* (blue triangles; black hexagon, type locality), *M. levis* (white circles; white star, type locality) and *Myloplus levis* morphologically distinct (orange diamond).

FIGURE 4. Morphological variation of *Myloplus levis*, ZUEC 6609, male, 141.5 mm SL.

FIGURE 5. *Myloplus tiete*, LBP 31564, (109406), 253.1 mm SL, Ilha Solteira municipality, rio Paraná.
FIGURE 6. *Myloplus tiete*, LBP 31564 (109401, 109404). **A**. Male, 256.1 mm SL, with second lobe well developed. **B.** Female 235.3 mm SL. Both from Ilha Solteira municipality, rio Paraná.
FIGURE 7. *Myloplus tiete*, MZUSP 12505, male, 168.3 mm SL, tomography. **A.** Frontal view of head. **B.** Dorsal view of the head. **C.** Lateral view of the entire body.

Figure 8. *Myloplus tiete*, NUP 13453, juvenile, 45.3 mm SL, Brazil, Mato Grosso do Sul, Taquarussu municipality, Rio Paraná.

FIGURE 9. *Myloplus levis*, LBP 12644(47119), female, 99.1 mm SL, Brazil, Corumbá municipality, rio Cuiabá, Paraguay basin.
FIGURE 10. Maximum likelihood tree of species of the group Myleinae *sensu* Kolmann *et al.* (2020), based on the COI gene (600pb). Bootstrap values of 100% are represented by the dark the nodes.

Tables

TABLE 1. Summary by species of new generated sequences used in the molecular analysis.

TABLE 2. Morphometric data of *Myloplus levis*. SD= standard deviation. The highlighted lines are morphometric data that differentiates *M. levis* from *M. tiete*.

TABLE 3. Morphometric data of *Myloplus tiete*. SD= standard deviation. The highlighted lines are morphometric data that differentiates *M. tiete* from *M. levis*.

Supplementary files

FIGURE S1. Radiography of Holotype of *Myloplus levis*, CAS 62107.

FIGURE S2. Photography of *Myloplus tiete*, previously deposited in IU, collected by H. von Ihering in Piracicaba, Brazil (CAS 12024, ex IU 10119).

FIGURE S3. Photography of the voucher specimen utilized by Mateussi *et al*. (2020) as *Myloplus levis*.

Tab S1. Summary by species of downloaded sequences used in the molecular analysis.

Espécie	GenBank	Tombo	Bacia	Coordenadas	Referência
Acnodon normani	MG751915.1	ISO1624	Xingu	3°22'04.0"S 51°59'58.9"W	Machado *et al*., 2018
Acnodon normani	MG751916.1	ISO1625	Xingu	3°22'04.0"S 51°59'58.9"W	Machado *et al*., 2018
Myleus setiger	MG752147.1	5480	Xingu	3°25'39.0"S 52°13'42.0"W	Machado *et al*., 2018
Myleus setiger	MG752155.1	14955	Aripuanã	7°17'19.8"S 60°38'10.0"W	Machado *et al*., 2018
Myleus setiger	MG752149.1	14067	Branco	2°47'58.3"N 60°40'00.1"W	Machado *et al*., 2018
Myloplus arnoldi	MG752167.1	1797	Xingu	5°45'19.1"S 57°21'13.2"W	Machado *et al*., 2018
Myloplus arnoldi	MG752186	15381	Tapajós	5°45'19.1"S 57°21'13.2"W	Machado *et al*., 2018
Myloplus arnoldi	MG752187.1	15383	Tapajós	5°45'19.1"S 57°21'13.2"W	Machado *et al*., 2018
Myloplus asterias	MG752239.1	15246	Madeira	3°41'15.5"S 59°57'01.3"W	Machado *et al*., 2018
Myloplus asterias	MG752240.1	15247	Madeira	3°41'15.5"S 59°57'01.3"W	Machado *et al*., 2018
Myloplus asterias	MG752241.1	15248	Madeira	3°41'15.5"S 59°57'01.3"W	Machado *et al*., 2018
Myloplus asterias	MG752206.1	12326	Negro	0°56'56.7"S 62°55'44.3"W	Machado *et al*., 2018
Myloplus asterias	MG752201	12220	Branco	0°58'08.5"S 61°54'02.2"W	Machado *et al*., 2018
Myloplus asterias	MG752220.1	14469	Nhamundá	1°41'27.1"S 57°25'20.1"W	Machado *et al*., 2018
Myloplus asterias	MG752251.1	UFPA - 1050353	Tocantins	6°34'01.2"S 51°01'57.0"W	Machado *et al*., 2018
Myloplus asterias	MG752252.1	UFPA - 1050353	Tocantins	6°34'01.2"S 51°01'57.0"W	Machado *et al*., 2018
Myloplus lobatus	MG752266	14293	Nhamundá	1°49'54.9"S 57°04'23.9"W	Machado *et al*., 2018
Myloplus lobatus	MG752282.1	100665	Jatapu	2°10'31.4"S 58°10'26.2"W	Machado *et al*., 2018
Myloplus lobatus	MG752289.1	107049	Japura	1°43'24.0"S 69°08'24.4"W	Machado *et al*., 2018

Myloplus lucienae	MG752295.1	P31536	Negro	2°43'02.5"S 60°44'41.5"W	Machado *et al*., 2018
Myloplus lucienae	MG752290.1	12347	Negro	0°19'31.7"S 64°08'04.1"W	Machado *et al*., 2018
Myloplus lucienae	MG752292.1	P29563	Negro	0°23'22.4"N 66°38'53.7"W	Machado *et al*., 2018
Myloplus nigrolineatus	MN702905.1	17153	Branco	1°33'12.2"N 61°15'26.8"W	Ota *et al*., 2020
Myloplus nigrolineatus	MN702904.1	15580	Negro	0°59'20.8"S 62°53'21.1"W	Machado *et al*., 2018
Myloplus nigrolineatus	MN702903.1	16865	Juruá	4°49'10.7"S 66°50'48.6"W	Machado *et al*., 2018
Myloplus aff rubripinnis	MG752359	12046	Branco	0°58'08.5"S 61°54'02.2"W	Machado *et al*., 2018
Myloplus aff rubripinnis	MG752226	14636	Negro	1°11'04.1"N 66°50'11.4"W	Machado *et al*., 2018
Myloplus aff rubripinnis	MG752227	14637	Negro	1°11'04.1"N 66°50'11.4"W	Machado *et al*., 2018
Myloplus torquatus	OR733049.1	620_TOC	Tocantins	7°05'06.0"S 47°36'46.8"W	Lima *et al*., 2024
Myloplus torquatus	OR733048.1	529_TOC	Tocantins	9°45'00.0"S 48°21'46.8"W	Lima *et al*., 2025
Myleus torquatus	OR733049.1	620_TOC	Tocantins	7°05'06.0"S 47°36'46.8"W	Lima *et al*., 2024
Myleus torquatus	OR733048.1	529_TOC	Tocantins	9°45'00.0"S 48°21'46.8"W	Lima *et al*., 2024
Myloplus tiete (*levis*)	MG752257.1	Rafa	Paraguai		Machado *et al*., 2018
Myloplus tiete (*levis*)	MG752258.1	Rafa2	Paraguai		Machado *et al*., 2018
Myleus tiete	MG752405.1	53243	Paraná	22°40'00.0"S 53°15'00.0"W	Machado *et al*., 2018
Myloplus zorroi	MG752408.1	14960	Aripuanã	7°17'19.8"S 60°38'10.0"W	Machado *et al*., 2018
Myloplus zorroi	MG752411	15144	Aripuanã	7°17'19.8"S 60°38'10.0"W	Machado *et al*., 2018
Myloplus zorroi	MG752414	15147	Aripuanã	10°09'46.5"S 59°26'54.9"W	Machado *et al*., 2018
Ossubtus xinguense	MG752461.1	11142	Xingu	3°50'27.0"S 52°41'46.0"W	Machado *et al*., 2018
Ossubtus xinguense	MG752463	11194	Xingu	3°27'28.0"S 51°42'30.8"W	Machado *et al*., 2018
Ossubtus xinguense	MG752465.1	11196	Xingu	3°27'28.0"S 51°42'30.8"W	Machado *et al*., 2018
Paramyloplus ternetzi	MZ052068.1	SU08-427	Suriname	3°11'54"N 55°24'27"W	Papa *et al*., 2021
Paramyloplus ternetzi	MZ052036.1	PAG-6265	Maroni	3°48'19"N 54°09'41"W	Papa *et al*., 2021

Paramyloplus ternetzi	MZ051909.1	PAG-6234	Maroni	3°48'19"N 54°09'41"W	Papa *et al*., 2021
Prosomyleus rhomboidalis	MG752325	1984	Xingu	3°50'27.0"S 52°41'46.0"W	Machado *et al*., 2018
Prosomyleus rhomboidalis	MG752334.1	14071	Branco	2°47'58.3"N 60°40'00.1"W	Machado *et al*., 2018
Prosomyleus rhomboidalis	MG752337.1	Jar211	Jari		Machado *et al*., 2018
Tometes makue	KX868697.1	INPA-43077	Negro		Ardura *et al*., 2009
Myloplus aylan 1		INPA-12648	Branco		Machado *et al*., 2024
Myloplus aylan 2		ANSP - 188823	Nanay		Machado *et al*., 2024
Myloplus aylan 3		180369			Machado *et al*., 2024
Myloplus aylan 4		22278			Machado *et al*., 2024
Myloplus schomburgkii		ANSP - 180812	Orinoco		Machado *et al*., 2024
Myloplus schomburgkii		1584	Tapajós		Machado *et al*., 2024
Myloplus schomburgkii		20768	Teles Pires		Machado *et al*., 2024
Myloplus sauron		P23608	Xingu		Machado *et al*., 2024
Myloplus sauron		P24617	Xingu		Machado *et al*., 2024
Myloplus sauron		P24618	Xingu		Machado *et al*., 2024